We are IntechOpen,
the world's leading publisher of
Open Access books
Built by scientists, for scientists

4,800
Open access books available

122,000
International authors and editors

135M
Downloads

Our authors are among the

154
Countries delivered to

TOP 1%
most cited scientists

12.2%
Contributors from top 500 universities

CLARIVATE ANALYTICS
BOOK CITATION INDEX
INDEXED

WEB OF SCIENCE™

Selection of our books indexed in the Book Citation Index
in Web of Science™ Core Collection (BKCI)

Interested in publishing with us?
Contact book.department@intechopen.com

Numbers displayed above are based on latest data collected.
For more information visit www.intechopen.com

Numerical Simulations
of Radiation and Scattering Characteristics
# of Dipole and LOOP Antennas

Oleg A. Yurtsev and Grigory V. Ptashinsky

Additional information is available at the end of the chapter

1. Introduction

Dipole and loop antennas are used in communication lines, in radar and navigation systems, TV and other fields of radio-engineering. Structures of antennas depend on their bandwidth. In VHF, UHF, L and S ranges, these antennas are made, as a rule, of conductors with a radius $A_o << \lambda$ (λ – wavelength in the air). Further, we will study wire dipole and loop antennas. Dipole and monopole antennas [Balanis, 1997; Markov, 1960], a Yagi-Uda antenna [Volakis, 2007; Aisenberg, Jampolsky and Terjoshin, 1977), bicone and discone antennas [Drabkin and Zuzenko, 1961], loop antennas consisting of one or two loops located in one plane [Rothammels, 1995] are well known. The length of a loop perimeter is $L \approx \lambda$. This ensures tuning of the antenna in resonance (a reactive part of input resistance is $X_r \approx 0$). To reduce sizes of dipole antennas, conductor with surface reactive resistance is used. Such a conductor can be implemented, for example, in the form of a cylindrical helix with a radius $A << \lambda$ [Yurtsev, Runov and Kazarin, 1974]. To tune antennas in resonance, reactive resistances are used. Linear arrays of dipole antennas with series excitation are described briefly [Rothammels, 1995].

In communication nodes and antenna arrays, dipole and loop antennas function in the conditions of strong coupling. Therefore, one of the problems of numerical simulation is the research into the influence of interaction on the electrical characteristics of antennas.

Scattering characteristics of antennas are a strong factor that facilitates radar reconnaissance. These characteristics of loop and dipole antennas have hardly been studied in the literature.

In the literature, there is no enough information or there is no information at all about a number of questions related to research into and the versions of construction of dipole and loop antenna. The following is related to these problems:

- optimization of dipole and loop antennas of complex shape according to various criteria (input resistance, directional pattern, bandness); Yagi-Uda multielement antennas, discone and bicone antennas, loop antennas with a quasi-isotropic directional pattern in the E-plane, a combination of loop and dipole antennas, all these antennas are attributed to complex antennas;
- arrays of dipole and loop antennas with series excitation;
- interaction of dipole and loop antennas in the near-field region;
- scattering characteristics of dipole and loop antennas.

The above specified questions are the contents of the present chapter.

2. Method of analysis and mathematical model of wire antenna

2.1. Integral and matrix equations to determine current in arbitrary thin conductor

Wire antennas are simulated numerically by the method of integral equations. In the present chapter, we have used Pockington's integral equation [Mittra, 1973]. The integral equation is solved by Galerkin method (method of the moments) [Harrington, 1968; Mittra, 1973; Fletcher, 1984]. To integrate the integral equation to a system of linear algebraic equations, impulse functions have been used further as basis and weight functions. In this case, the basic part of each matrix coefficient of this system is defined by an exact analytical expression. That ensures the enhancement of accuracy of solution of the integral equation and reduces this problem time.

According to [Mittra, 1973], Pockington's integral equation looks like:

$$Z_s(l_p) \cdot I(l_p) + Z_l(l_p) \cdot I(l_p) + \int_0^L I(l_q) Z(l_p, l_q) dl_q = U(l_p), \tag{1}$$

where

$I(l_q)$ is the sought current that flows in a conductor under the influence of an extraneous field, which excites the conductor;
$Z_s(l_p) = R_s + iX_s$ is the surface resistance of a conductor;
$Z_l(l_p)$ is the lumped complex impedance connected to the rupture of an antenna conductor – a load;
L is the conductor length.

The kernel of the integral equation $Z(l_p, l_q)$ is defined by the expression:

$$Z(l_p, l_q) = -i30k \left[G(l_p, l_q) \cdot (\vec{l}_o, \vec{S}_o) - \frac{1}{k^2} \frac{d^2 G(l_p, l_q)}{dl_p dl_q} \right]. \tag{2}$$

The right side depends on distribution of the extraneous field that excites the conductor:

$$U(l_p) = -(\vec{E}_{os}(l_p), \vec{l}_o),$$ (3)

where $i = \sqrt{-1}$; $k = \dfrac{2\pi}{\lambda}$ is the wave number of free space, λ is the wavelength of the field that excites the conductor;

$\vec{E}_{os}$ is the vector of the extraneous electric field that excites the conductor.

Green's function is defined by the expression:

$$G(l_p, l_q) = \frac{e^{ikR}}{R}.$$ (4)

The remaining quantities included in (1) – (4) are shown in fig. 1.

When solving an integral equation by the method of moments, a conductor of arbitrary shape is divided into M rectilinear segments of length $\Delta L \ll \lambda$. Coordinates of the beginning ($X1_m, Y1_m, Z1_m$) and the end ($X2_m, Y2_m, Z2_m$) of each segment are calculated (m is the segment number, $1 \le m \le M$).

The use of impulse basis and weight functions leads to the following system of linear algebraic equations:

$$Z_{sn} + Z_{lk} + \sum_{m=1}^{M} I_m K_{mn} = U_n,$$ (5)

where

M is the number of segments, into which the whole conductor of length L is divided;
m is the number of a segment, in which point Q (source point) is located (fig. 1), $1 \le m \le M$;
n is the number of a segment, in which point P (point of observation) is located (fig. 1), $1 \le n \le M$;
Z_{sn} is the surface resistance in a segment with number n;
Z_{lk} is the series load resistance of a conductor, k is the number of a segment, to which the resistance is connected;
I_m is the sought current in a segment with number m.

The matrix coefficients are determined by the expression:

$$K_{mn} = \int_{\Delta L_n} \int_{\Delta L_m} \left[Z(l_p, l_q)(\vec{l}_{on}, \vec{S}_{om}) \right] dl_q dl_p = A_{mn} + B_{mn},$$ (6)

where

$\Delta L_n, \Delta L_m$ are the lengths of segments with numbers n and m;
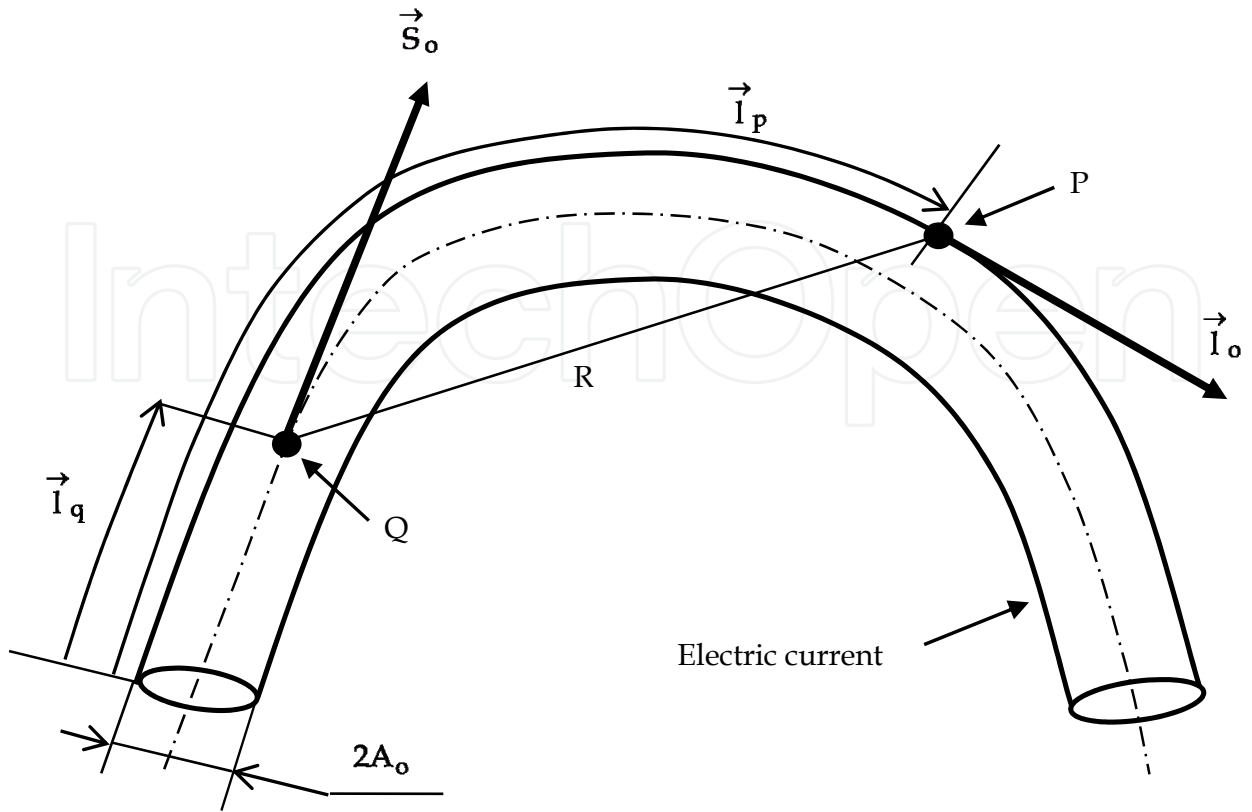$\vec{l}_{on}, \vec{S}_{om}$ are unit vectors, tangent to a conductor in the centre of segments with numbers n and m;

Figure 1. Conductor model

$$A_{mn} = -i30k \int\limits_{Z_{n1}}^{Z_{n2}} \int\limits_{Z_{m1}}^{Z_{m2}} G(z_p, z_q) dz_q dz_p ; \qquad (7)$$

$$B_{mn} = i\frac{30}{k}[G_{22} - G_{12} - G_{21} + G_{11}]; \qquad (8)$$

$$G_{22} = \frac{e^{ikR_{22}}}{R_{22}}; \quad G_{12} = \frac{e^{ikR_{12}}}{R_{12}}; \qquad (9)$$

$$G_{21} = \frac{e^{ikR_{21}}}{R_{21}}; \quad G_{11} = \frac{e^{ikR_{11}}}{R_{11}}; \qquad (10)$$

$$R_{22} = \sqrt{(X_{n2} - X_{m2})^2 + (Y_{n2} - Y_{m2})^2 + (Z_{n2} - Z_{m2})^2 + a_o^2} ; \qquad (11)$$

$$R_{12} = \sqrt{(X_{n1} - X_{m2})^2 + (Y_{n1} - Y_{m2})^2 + (Z_{n1} - Z_{m2})^2 + a_o^2} ; \qquad (12)$$

$$R_{21} = \sqrt{(X_{n2} - X_{m1})^2 + (Y_{n2} - Y_{m1})^2 + (Z_{n2} - Z_{m1})^2 + a_o^2} ; \qquad (13)$$

$$R_{11} = \sqrt{(X_{n1} - X_{m1})^2 + (Y_{n1} - Y_{m1})^2 + (Z_{n1} - Z_{m1})^2 + a_o^2} \ . \tag{14}$$

The right side of the system of equations (5) according to (3) turns out to be equal to:

$$U_n = -\int_{\Delta L_n} (\vec{E}_{os}, \vec{1}_{on}) f_n(l_p) dl_p \ . \tag{15}$$

The weight function is distinct from zero and is equal to unity only within a segment with number n. Therefore, it follows from (15) that:

$$U_n = -\int_{\Delta L_n} E_{\tau n}(l_p) dl_p = |U_n| \exp(\Psi_n), \tag{16}$$

where

$E_{\tau n}$ is the component of an extraneous field, tangent to a conductor in a segment with number n;

$|U_n|$, Ψ_n are the amplitude and the phase of an exciting voltage in a segment with number n.

The further transformation into (16) is different for radiation and scattering problems.

2.2. Radiation problem

When solving a radiation problem, the extraneous field is considered to be distinct from zero only in the space of excitation and constant as for its amplitude and phase within the space. In this case, it follows from (16) that:

$$U_n = -U, \tag{17}$$

where

U is the excitation voltage;

$U_n \neq 0$ only in those segments, which are within the space of excitation. It means that, in the system of equations (5), the right side is given in accordance with (17) in the equations, the numbers of which correspond to the numbers of segments within the space of excitation.

As a result of numerical solution of the system of linear algebraic equations (5), the current in each segment I_m is found. The amplitude and the initial phase of the current within each segment is considered to be constant. According to the current distribution in a conductor and the given voltage U, the input resistance $Z_{inp} = R_{inp} + iX_{inp}$ is determined,

where

$$Z_{inp} = \frac{U_{inp}}{I_{inp}}, \tag{18}$$

U_{inp}, I_{inp} are the input voltage and the input current. The input voltage is the given voltage U in the space of excitation. The input current is the current at the ends of the segment (segments) that fills (fill) the space of excitation in a conductor model. The situation is explicated by fig. 2 that shows a part of a conductor of an antenna and some segments.
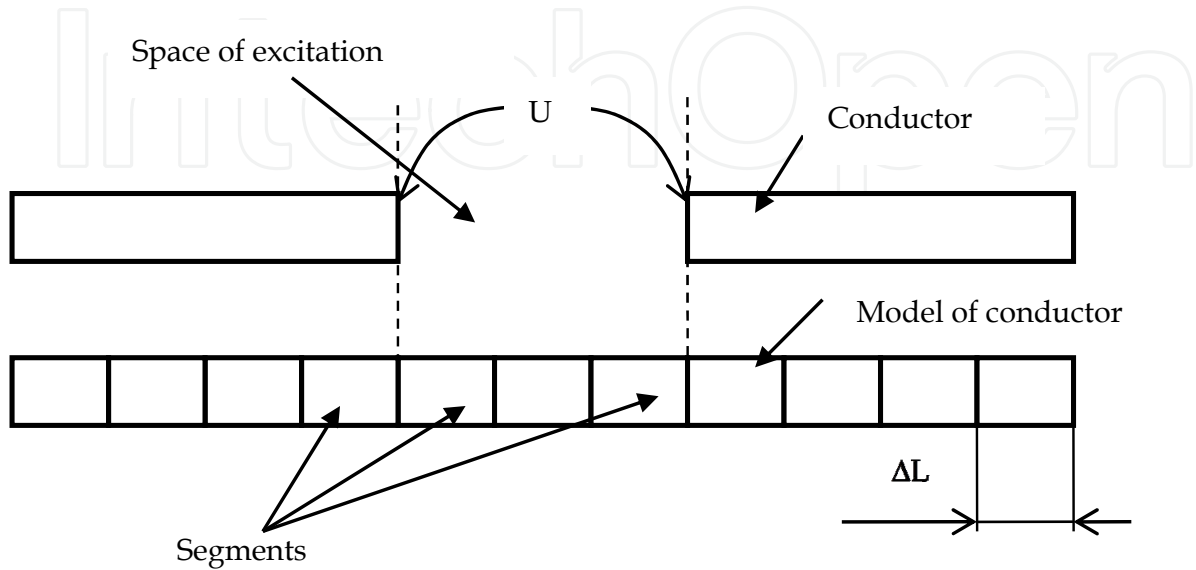

Figure 2. Conductor and its model

If there is one segment in the space of excitation, $I_{inp} = I_{n_o}$ is the current in a segment of excitation, n_o is the number of a segment of excitation. The current in each segment is the complex quantity $I_{inp} = \text{Re}(I_{inp}) + i\,\text{Im}(I_{inp})$. Therefore, $Z_{inp} = R_{inp} + iX_{inp}$, where R_{inp} and X_{inp} are the active and reactive parts of input resistance of the antenna:

$$R_{inp} = U \frac{\text{Re}(I_{inp})}{\left|I_{inp}\right|^2}: \quad X_{inp} = -U \frac{\text{Im}(I_{inp})}{\left|I_{inp}\right|^2} \tag{19}$$

According to the found current distribution in the conductor, the geometry of the conductor, it is easy to determine numerically the conductor field in space in any zone, and further, the basic characteristics and parametres of a wire antenna: its directional pattern, phase diagram, polarization pattern, directivity factor. These questions compose the contents of an exterior problem of the theory, it will be studied in more detail below.

2.3. Scattering problem

The mathematical model of a wire antenna in the scattering mode includes the above relationships that determine current in scattering conductors, and the expression that defines the right side of the matrix equation (3). We will study (3) for the case of excitation of a conductor by a plane wave falling from the given direction. The problem is explicated by fig. 3.

The figure shows a scattering conductor in the X, Y, Z coordinate system, vectors $\vec{E}_i$ $\vec{H}_i$ of a field of an incident wave, vector $\vec{\Pi}_i$ of power flux density of an incident wave. The direction of the incident wave propagation is set by an angle θ_i that is the angle between the Z axis and vector $\vec{\Pi}_i$. The wave field $\vec{E}_i$, $\vec{H}_i$ is extraneous, and $\vec{E}_{os} = \vec{E}_i$. In general, the vector $\vec{E}_i$ and the unit vector $\vec{l}_o$ in the expression (3) have three orthogonal components:

$$\vec{E}_i = E_{ix} \cdot \vec{x}_0 + E_{iy} \cdot \vec{y}_0 + E_{iz} \cdot \vec{z}_0 ,\tag{20}$$

where E_{ix}, E_{iy}, E_{iz} are the complex amplitudes of the vector $\vec{E}_i$ components;

$$\vec{l}_o = \vec{x}_0 \cos\alpha_x + \vec{y}_0 \cos\alpha_y + \vec{z}_0 \cos\alpha_z ,\tag{21}$$

where $\cos\alpha_x$ $\cos\alpha_y$ $\cos\alpha_z$ are the direction cosines of the vector $\vec{l}_o$ in relation to the X, Y, Z coordinate axes;
$\vec{x}_o$, $\vec{y}_o$, $\vec{z}_o$ are the unit vectors of the coordinate system of X, Y, Z.
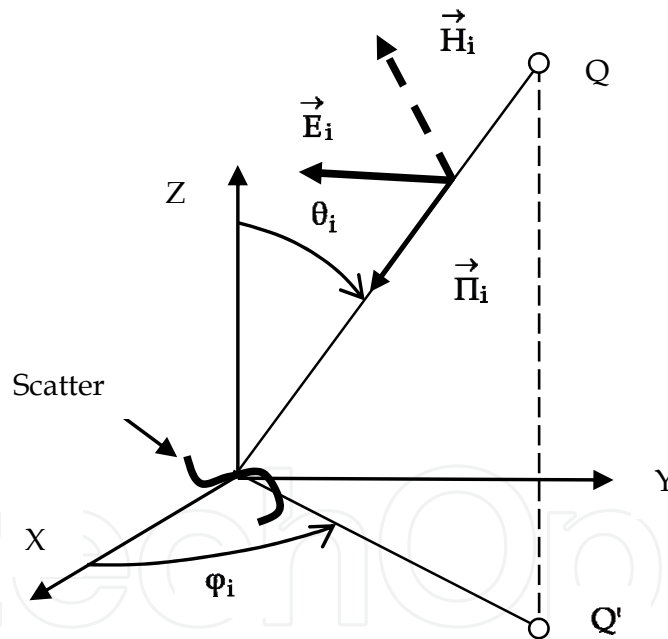
Figure 3. Scatterer conductor in space

It follows from (3), (20), (21) that:

$$U(l_p) = E_{ix}(l_p) \cdot \cos\alpha_x + E_{iy}(l_p) \cdot \cos\alpha_y + E_{iz}(l_p) \cdot \cos\alpha_z .\tag{22}$$

If the antenna is irradiated by a plane electromagnetic wave, the amplitude of the electric field is the same at all the points of the antenna and equal to E_{io}. In this case, in the expression (20):

$$\left|E_{ix}(l_p)\right| = E_{io}\cos\theta_i\sin\varphi_i;\ \left|E_{iy}(l_p)\right| = E_{io}\cos\theta_i\cos\varphi_i;\ \left|E_{iz}(l_p)\right| = E_{io}\sin\theta_i, \tag{23}$$

where θ_i φ_i are the angular coordinates of a transmitter of an irradiating electromagnetic wave located at point Q (see fig. 3, angle φ_i is calculated from the X axis to the Y axis).

The phase $U(l_p)$ in a segment with number m depends on the segment position in space, and is determined by the expression:

$$\Psi_m = -k(X_m\cos\theta_i\cos\varphi_i + Y_m\sin\theta_i\sin\varphi_i + Z_m\cos\theta_i), \tag{24}$$

where X_m, Y_m, Z_m are the coordinates of the centre of the segment with number m.

2.4. Radiation (scattered) field of thin conductor

The field at an arbitrary point of space P is determined according to the found current distribution $I(l_q)$ in a conductor. The positon of the point P is set by spherical coordinates R, θ, φ - fig. 4. To calculate the electric field at the point P, the vector-potential method has been used [Stratton, 1941; Volakis, 2007]:

$$\vec{E} \approx -i\frac{60\pi}{\lambda}\int_L I(l_q)\cdot\vec{S}_o\frac{e^{-kR_{pq}}}{R_{pq}}dl_q, \tag{25}$$

where R_{pq} is the distance from point of observation P to point Q on the antenna (see fig. 1).
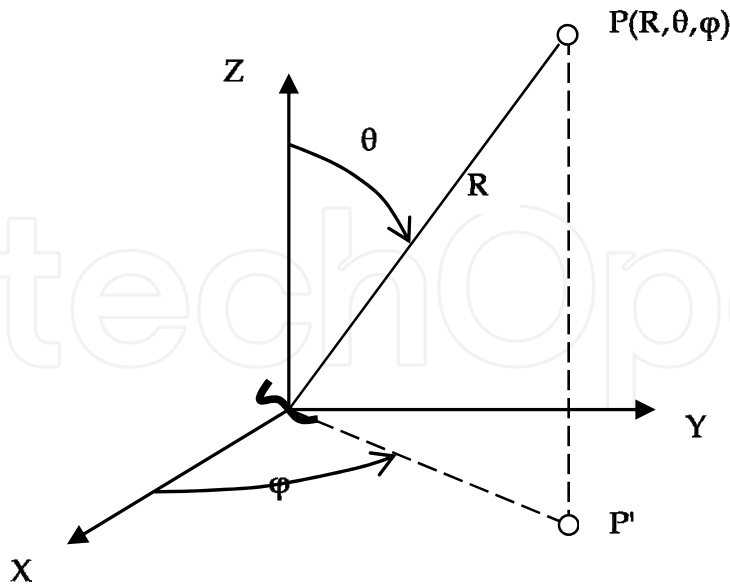
Figure 4. Point of observation in space

When calculating the current $I(l_q)$, all the antenna conductors are divided into rectilinear segments of length $\Delta L \ll \lambda$. The current amplitude $\left|I_m\right|$ and the current phase Ψ_m are

considered to be constant within each segment with number m. Therefore, the integral (25) is transformed into the sum of fields of M segments:

$$\vec{E} \approx E_o \sum_{m=1}^{M} I_m \vec{S}_{om} \frac{e^{-kR_m}}{R_m}. \tag{26}$$

where $E_o = -i60\pi \cdot \Delta L / \lambda$; R_m is the distance from a segment with number m to point P:

$$R_m = \sqrt{(X_m - X_p)^2 + (Y_m - Y_p)^2 + (Z_m - Z_p)^2}, \tag{27}$$

$\vec{S}_{om}$ is the unit vector, tangent to a conductor in a segment with number m.

Vectors $\vec{S}_{om}$ and $\vec{E}$ are represented in the form of the sum of projections on the X, Y, Z axes:

$$\vec{S}_{om} = \frac{X_{m2} - X_{m1}}{\Delta L} \vec{x}_o + \frac{Y_{m2} - Y_{m1}}{\Delta L} \vec{y}_o + \frac{Z_{m2} - Z_{m1}}{\Delta L} \vec{z}_o, \tag{28}$$

$$\vec{E} = E_x \vec{x}_o + E_y \vec{y}_o + E_z \vec{z}_o. \tag{29}$$

The cross components E_θ and E_φ can be expressed by the projections E_x, E_y, E_z:

$$\begin{aligned} E_\theta(\theta,\varphi) &= -E_z \sin\theta + (E_x \cos\varphi + E_y \sin\varphi)\cos\theta, \\ E_\varphi(\theta,\varphi) &= -E_x \sin\varphi + E_y \cos\varphi. \end{aligned} \tag{30}$$

2.5. Directional pattern, directivity factor and gain

The directional pattern $F(\theta,\varphi)$ is determined by a field of the antenna in the radiation mode, the scattering pattern $F_s(\theta,\varphi)$ is determined by the field in the scattering mode. The fields in the radiation and scattering modes are described by the same expressions (30). Therefore, the directional pattern and the scattering pattern of the antenna are determined by the same expression:

$$F(\theta,\varphi) = E(\theta,\varphi) / E_{max} = F_s(\theta,\varphi), \tag{31}$$

where E_{max} is the maximum value of a field on a sphere $R = const$.

The shape of $F(\theta,\varphi)$ and $F_s(\theta,\varphi)$ is different, as the current distribution is different in antenna conductors in the radiation and scattering modes.

The directivity factor (D) is determined by a directional pattern [Balanis; Aisenberg, Jampolsky and Terjoshin, 1977]:

$$G = \frac{4\pi}{\int_{\varphi=0}^{2\pi} \left[\int_{\theta=0}^{\pi} F^2(\theta,\varphi)\sin\theta \cdot d\theta \right] d\varphi}. \tag{32}$$

The antenna gain (G) characterises the antenna directional properties and power heat loss in antenna elements [Mittra, 1973]:

$$G = R^2 \frac{E_{max}^2}{30U_{inp} \cdot I_{inp}} . \tag{33}$$

2.6. Radar Cross Section

The radar cross section (RCS) of antennas can exceed considerably the effective area of an object, on which the antennas are installed. That is why it is necessary to take into consideration the scattering properties of the antenna, when developping countermeasures to radar reconnaissance. In accordance with [Crispin and Maffett, 1965; Scolnic, 1970;]

$$S = 4\pi R^2 \left| \frac{E}{E_i} \right|^2 , \tag{34}$$

where

S is the radar cross section;

R is the distance from an antenna to a point of observation in space;

E is the amplitude of a scattered field in the point of observation;

E_i is the amplitude of the electric field of an irradiating wave in the place of antenna location.

The scattering pattern and RCS depend on the antenna structure, frequency, polarization, and direction of falling of an electromagnetic wave on the antenna. RCS is described in general by the polarization scattering matrix:

$$S = \begin{vmatrix} S_{\theta\theta} & S_{\theta\varphi} \\ S_{\varphi\theta} & S_{\varphi\varphi} \end{vmatrix} , \tag{35}$$

where

$S_{\theta\theta}$ is the RCS calculated according to a scattered field component E_θ, when the object is irradiated by a field $E_{i\theta}$;

$S_{\theta\varphi}$ is the RCS calculated according to a scattered field component E_θ, when the object is irradiated by a field $E_{i\varphi}$;

$S_{\varphi\theta}$ is the RCS calculated according to a scattered field component E_φ, when the object is irradiated by a field $E_{i\theta}$;

$S_{\varphi\varphi}$ is the RCS calculated according to a scattered field component E_φ, when the object is irradiated by a field $E_{i\varphi}$.

The scattered field and RCS of the antenna can be represented as the sum of two components: antenna component S_a and structural component S_s [Sazonov and

Shkolnikov, 1974]. The irradiating wave creates conduction currents in the antenna conductors. These currents radiate the field that is a structural component of the scattered field. The RCS corresponding to this field is S_s. At the same time, the antenna currents excite the transmission line connected to the antenna. The wave in the transmission line is reflected from a load and is radiated by the antenna. This scattered field is the antenna component. The RCS corresponding to this field is S_a. If the load is matched to the transmission line, S_a =0. The antenna components and the structural components of the scattered field differ from each other not only by their scattering pattern, but by their phase diagram as well. Therefore, after having determined separately the components S_a, S_s and the scattered fields corresponding to these components, it is impossible to found the total RCS as their arithmetical sum [Crispin and Maffett, 1965]. The antenna component of the RCS is related to an antenna gain and a VSWR in the transmission line. When calculating the RCS by the formula (34), it is necessary to connect the matched load to the antenna port. Such an oppotunity is provided in the integral equation (1). The number of the segment k, to which the load Z_{lk} is connected, shall coincide with the number of a segment of excitation.

The scattering pattern differs from the directional pattern (DP) of an antenna in the transmission (reception) mode. It is related to the fact that a structural component predominates over an antenna component in a scattered field. The structural component of the scattered field is the result of radiation of the currents created by an incident EMW in the antenna. Distribution of these currents can differ essentially from current distribution in the antenna in the transmission mode.

2.7. Interaction of antennas located in near-field region

An integral equation and the subsequent part of a mathematical model of a wire antenna allow modelling wire antennas with an arbitrary geometry, located in the near-field region. If several antennas are located in the near-field region, the length L is the total length of conductors of all the antennas. If, in the radiation mode, only one antenna from group functions (an active antenna), and entries of all the remaining antennas are loaded with matched loads (passive antennas), it is possible to determine an isolation ratio between the active antenna and every other passive antenna. The isolation ratio of a field is calculated as the ratio of complex amplitudes of currents at the entry of the active antenna $(I_{inp})_a$ and a passive antenna $(I_{inp})_p$. The power isolation ratio K_p is equal to:

$$K_p = \left| \frac{(I_{inp})_a}{(I_{inp})_p} \right|^2 .$$

(36)

The described mathematical model has been used in the program, with the help of which the results below have been obtained.

3. Modelling of radiation and scattering characteristics of dipole antennas

3.1. Dipole antennas and Yagi-Uda antenna

Fig.5 shows a Yagi-Uda antenna. Antenna elements: 1 is a linea reflector; 2 is a dipole; 3 are directors. Plane and corner reflectors are used too(see fig. 6). The polarization of the antenna is linear. Plane XZ is E-plane; plane YZ is H-plane. According to fig. 4, in XZ-plane φ =0, in YZ-plane φ =90°.
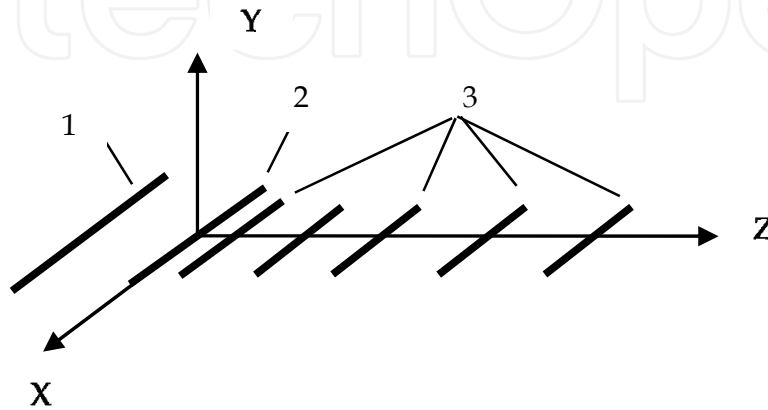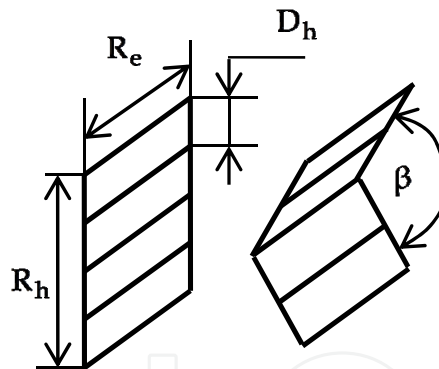

Figure 5. Yagi-Uda antenna

Figure 6. Versions of reflectors

The antenna is optimised as for its input resistance, gain, backscattered radiation level («Front to back» parameter: F/B). Its directional pattern, input resistance, directivity factor, gain depend on the antenna geometrical parametres, frequency, the surface resistance of conductors and the connected lumped resistances. Further, all the regularities are illustrated by the example of antennas intended for a medium frequency f=300 MHz. Size values of the antenna elements are not shown because of the lack of space.

3.1.1. Radiation characteristics

Fig. 7 shows the dependence of a directivity factor (D) of the relations F/B on the number of directors (N). The antenna reflector is linear. For each N value, sizes of the antenna

elements are selected so that the input resistance was equal to $R_{inp} \approx 50$ Ohm, $X_{inp} \approx 0$. The results have been obtained for the case Z_s =0. Fig. 8 shows (as an example) a directional pattern in the E-plane at N=10. Fig. 9 shows the dependences of gain and «Front to Bback» ratio (F/B) on the reflector sizes in the H-plane at a different distance between conductors of the reflector: D_h =0,05 λ = 50 mm and D_h =0,1 λ = 100 mm; fig. 10 shows the dependence of G and F/B on the reflector size in the E-plane.

It follows from the cited and other results of simulation that the antenna gain and input resistance depend little on reflector sizes. If R_e changes in the interval $(0,2 … 1)\lambda$, the active input resistance varies in the interval (48,5 … 50) Ohm, and the reactive input resistance varies in the interval (0 …-1,7) Ohm. If the distance between the conductors of the reflector is D_h <0,1 λ, the antenna parametres hardly depend on Dh. The maximum of the F/B parametre corresponds to $R_e \approx R_h \approx (0,6 … 0,7)$ λ.
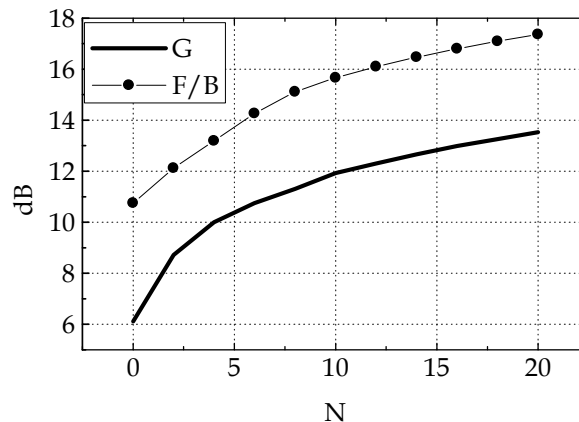
Figure 7. Gain and Front to Back ratio
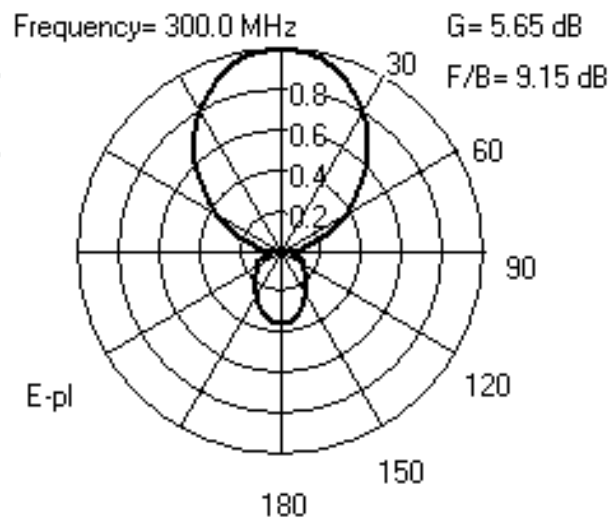
Figure 8. Radiation pattern
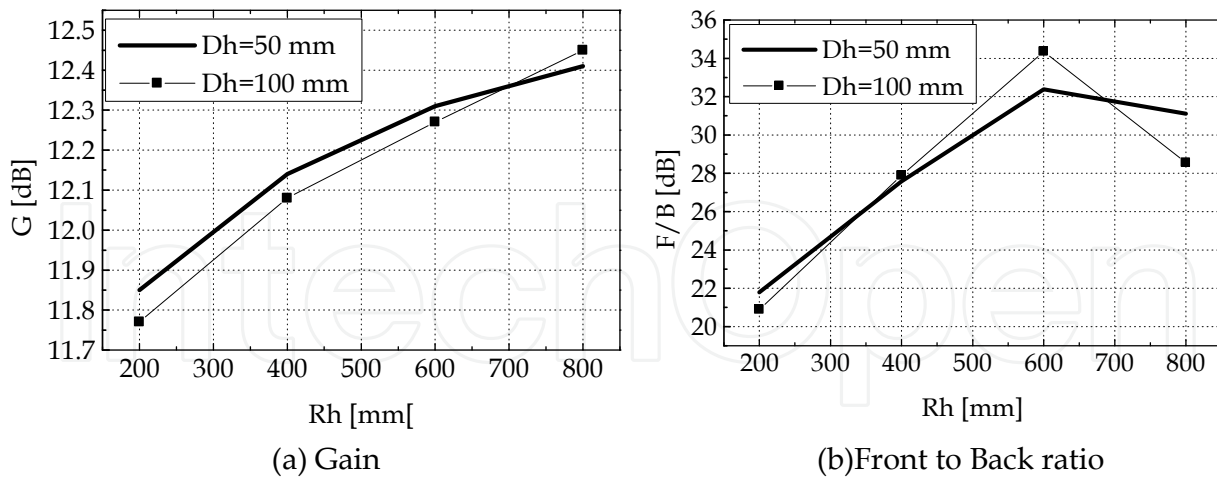
Figure 9. Dependence of Gain (G) and Front to Back ratio (F/B) on reflector size in H-plane

The graph in fig. 11 illustrates the influence of shape of a reflector on the antenna parametres. The dependences of G and F/B on an angle β are shown for the reflector sizes $R_e = R_h = 0{,}6\ \lambda = 600$ mm, $D_h = 0{,}1\ \lambda$ and N=10. It follows from fig. 11 that when an angle β decreases, the F/B parametre worsens, and that the gain hardly depend on β. When β increases, the input resistance increases.

3.1.2. Scattering characteristics

By the example of a dipole, it is convenient to show the dependence of current distribution in the scattering mode on the direction of radiation. Fig. 12 shows current distribution in a dipole with nonresonant length L=1,25λ. The dipole is irradiated from the direction that is perpendicular to the dipole axis (along the Z axis, see fig. 5), and at an angle of 45° to the axis. Fig. 13 shows the corresponding scattering patterns in the E-plane. The figures give the values of $RCSN = RCS\,/\,\lambda^2$ in the direction of a maximum of the scattering pattern.
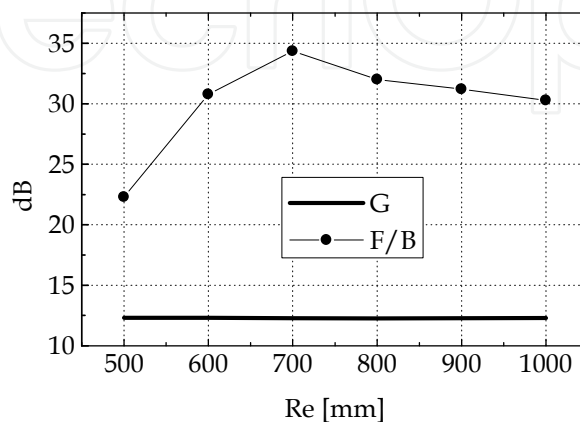
Figure 10. Dependence of G and F/B on reflector size in E-plane
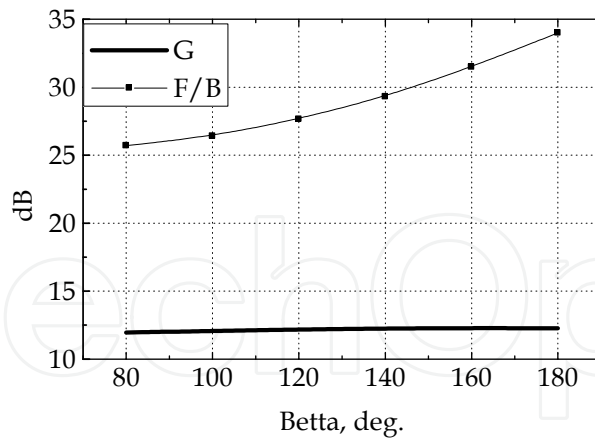
Figure 11. Dependence of G and F/B on angle β
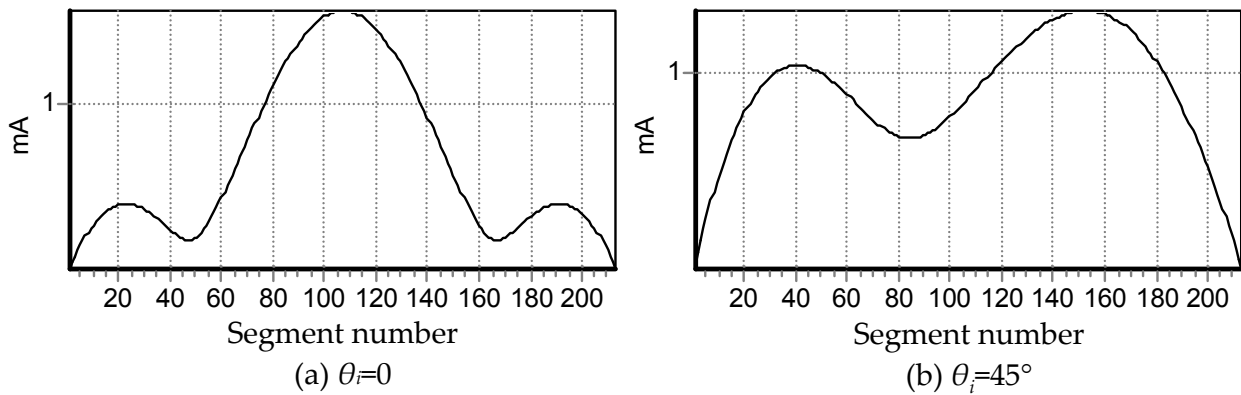
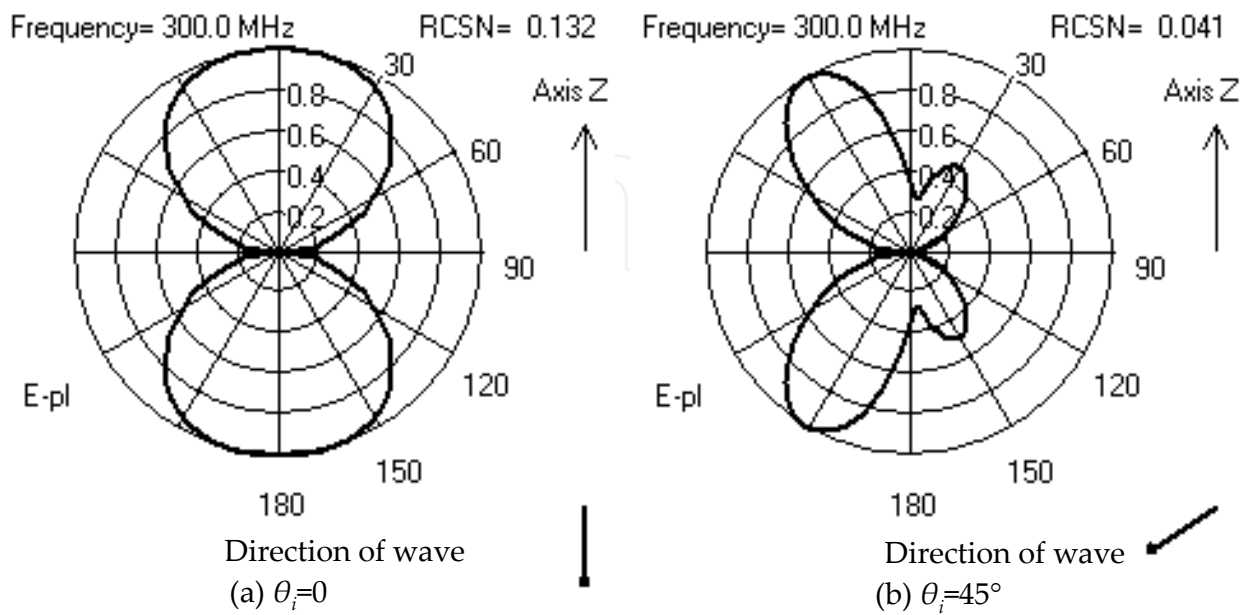**Figure 12.** Current distribution

Figure 13. Scattering pattern of dipole

Fig. 14 illustrates the difference of a directional pattern and a scattering pattern and the dependence of the scattering pattern on the direction of propagation of an irradiating wave in relation to the antenna axis (Z axis). The calculations have been made for a Yagi-Uda antenna with a linear reflector, frequency f=300 MHz, N=10.
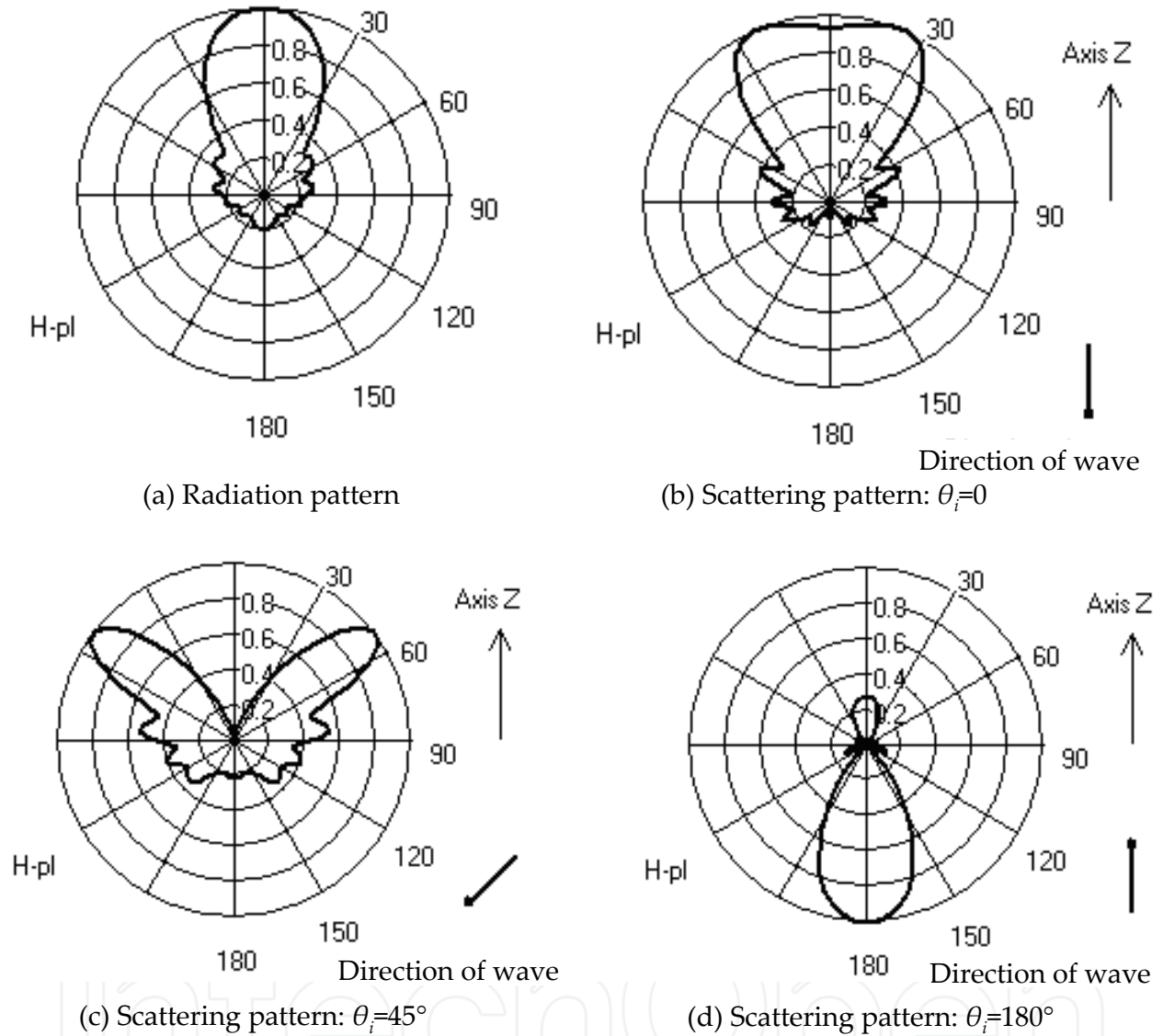

(a) Radiation pattern

(b) Scattering pattern: θ_i=0

(c) Scattering pattern: θ_i=45°

(d) Scattering pattern: θ_i=180°

Figure 14. Radiation pattern (a) and scattering pattern (b, c, d)

Fig. 15 shows the dependence of RCSN in the direction of a maximum of the scattering pattern on the number of directors N. The calculation has been made for the matched load of the antenna $Z_l = Z_{inp}^*$ and for the short-circuit load ($Z_l = 0$). It follows from fig. 15 that a structural component of RCS is much more bigger, than its antenna component.

3.1.3. Dipole antennas with reduced dimensions

In case of increase of a surface inductive reactance X_s, resonance frequency f₀ of an antenna decreases. The most practical version of implementation of the surface resistance is the

application of, instead of a smooth conductor, a conductor rolled into a helix with a radius A_o, fig. 16. The surface resistance is the ratio of the tangential components of vectors $\vec{E}$ and $\vec{H}$ of the helix field on a cylinder of the radius A_o, namely $Z_s = R_s + iX_s = E_t / H_t$.
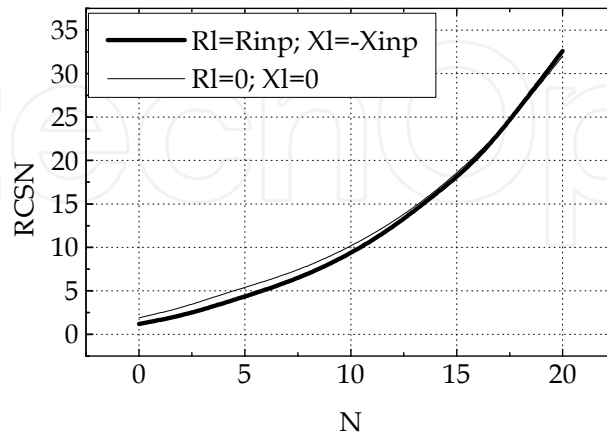

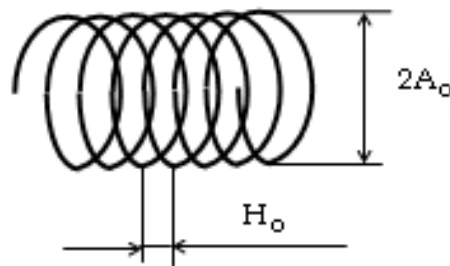**Figure 15.** Dependence of RCSN on number of directors

Figure 16. Helix

For the case $A_o \ll \lambda$, the reactance X_s turns out to be equal to [Yurtsev, Runov, Kazarin 1974]:

$$X_s \approx 480\pi^4 \left(\frac{A_o}{\lambda}\right)\left(\frac{A_o}{H_o}\right)^2 [\text{Ohm}]. \tag{37}$$

The more the ratio A_o / H_o, the more X_s and the less the antenna resonance frequency. Fig. 17 shows the dependence R_{inp} and X_{inp} on frequency at two values of A_o for a dipole tuned in resonance at a frequency of 300 MHz at $X_s = 0$.

In case of decrease of Ho and $Ao = const$, the resonance frequency and a frequency band according to a matching criterion decreases. Fig. 18 shows the dependence of a resonance frequency f_o for a Yagi-Uda antenna with a linear reflector and one director, depending on Ho at $A_o = 0,003\lambda = 3$ mm. The antenna of a smooth conductor with a radius $A_o = 3$ mm was tuned to a frequency of 300 MHz. In case of decrease of Ho, the resonance frequency f_o decreases, the band properties worsen, the F/B parametre decreases, the antenna gain G decreases. Fig. 19 shows the dependence of the percentage bandwidth df / f_o, in which

VSWR <2 (the antenna input resistance at a medium frequency f_o is equal to R_{inp} =50 Ohm, X_{inp} =0, the wave resistance of a feeder is ρ =50 Ohm).
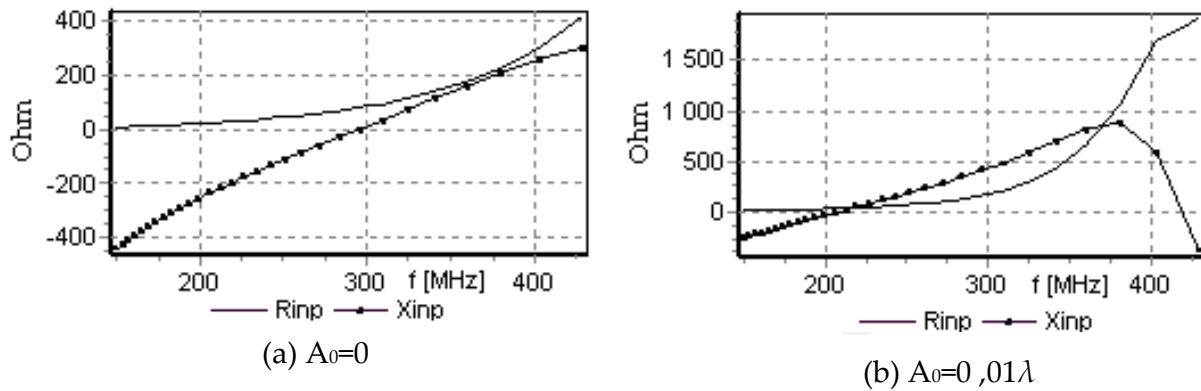

(a) A0=0

(b) A0=0 ,01λ

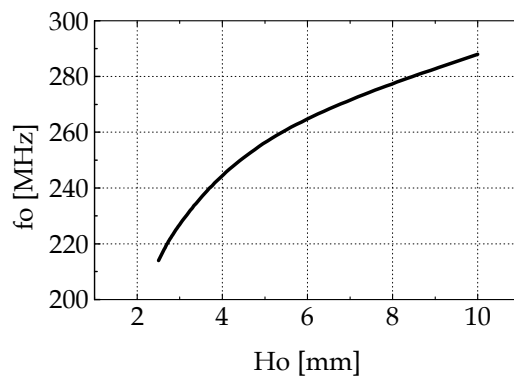**Figure 17.** Dependence of input resistance on frequency at $H_o = 0,01\lambda$
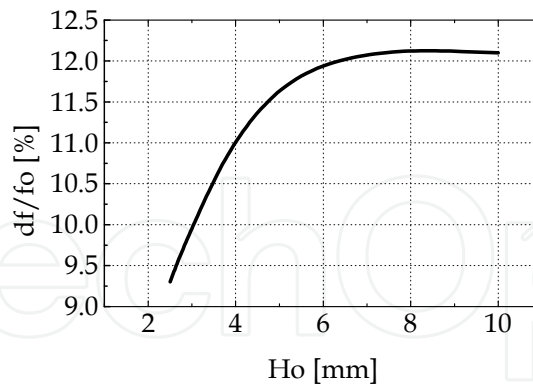

Figure 18. Resonance frequency

Figure 19. Percentage bandwidth

In case of change of H_o from 10 mm to 2.5 mm, G decreases from 7 dB to 5 dB, F/B decreases from 20 dB to 14 dB.

3.2. Flat and convex dipole and Yagi arrays

One of the main questions of the numerical analysis of antenna arrays and antennas as a part of a group in the near-field region is the question of interaction of antennas. The

coupling effect of antennas, located in a near-field region, results in changes of all the characteristics of the antennas. Further, the differences in interaction between emitters in plane and convex arrays have been studied by the example of comparison of linear and arc arrays. The interaction of two Yagi-Uda antennas has also been studied, depending on a distance between them and their cross orientation. It is important for the organisation of communication nodes.

The received regularities are illustrated by the example of a Yagi-Uda antenna with the number of directors N=1. The antenna is tuned so that the input resistance is equal to 50 Ohm at a medium frequency of 300 MHz.

Fig. 20 shows directional patterns of the antenna located at the centre of a fragment of a plane array with the number of emitters N_x on the X axis, and N_y on the Y axis. The distances between the emitters on the X, Y axes are equal to 0,55 λ. It ensures the absence of diffraction maximums in the directional pattern at the phase scanning in a sector of $\pm 40°$. All the emitters of the fragment, except for the central one, are loaded with matched loads. The numerical simulation shows that, with the increase of the number of the emitters in the fragment, the shape of the directional pattern in some angular sector tends to become right-angled. The degree of interaction of two emitters between themselves can be evaluated by the isolation ratio $S12 = (I_1 / I_2)^2$, where I_1 is the amplitude of an input current of an emitter in the radiation mode, I_2 is the amplitude of an input current of a passive emitter loaded with a matched load. Fig. 22 shows the dependence $S12$ on $R' = R / \lambda$, where R is the distance between emitters. The calculations have been made for a Yagi-Uda antenna at the number of directors N=1 and N=5 with the location of antennas in the E-plane and the H-plane. It follows from the simulation results that $S12$ depends little on the number of directors. If the antennas are located in the H-plane, the interaction is stronger. If the distance is $R > \lambda$, the interaction of the antennas is negligible. It means that it is sufficient to take into consideration the interaction of a Yagi-Uda antenna as a part of a plane array only with an environment of two rings.
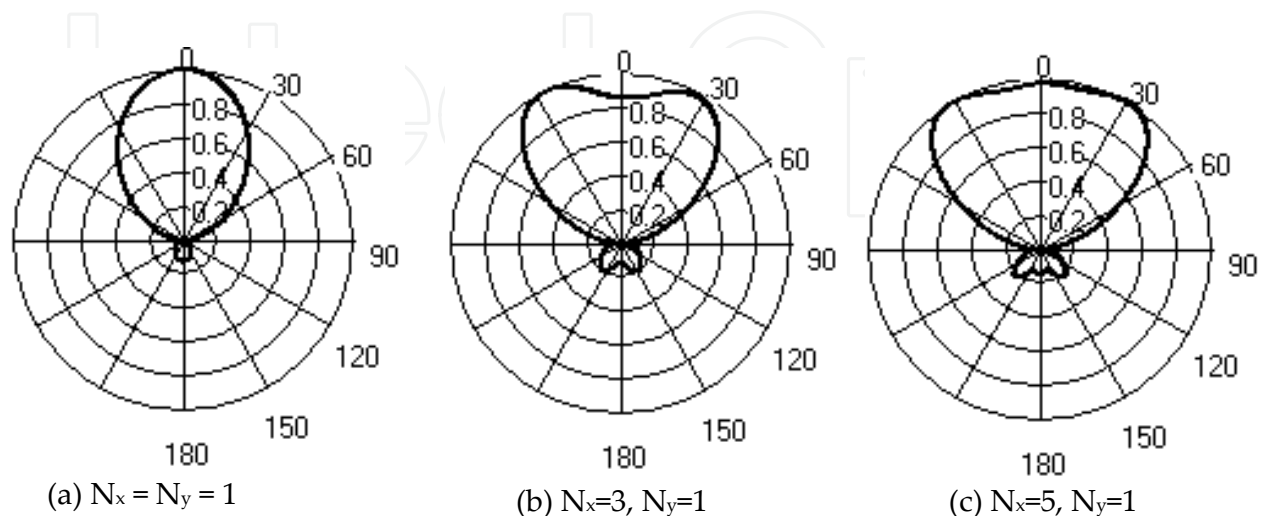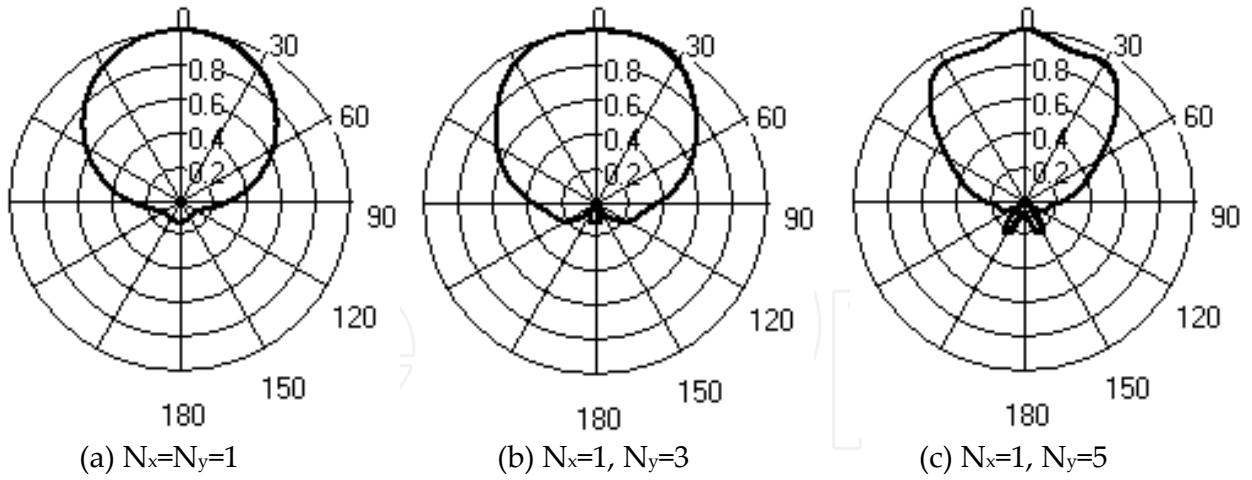

(a) $N_x = N_y = 1$ (b) $N_x=3$, $N_y=1$ (c) $N_x=5$, $N_y=1$

Figure 20. Radiation pattern in E-plane

(a) $N_x=N_y=1$ (b) $N_x=1$, $N_y=3$ (c) $N_x=1$, $N_y=5$

Figure 21. Radiation pattern in H-plane

(a) N=1   (b) N=5
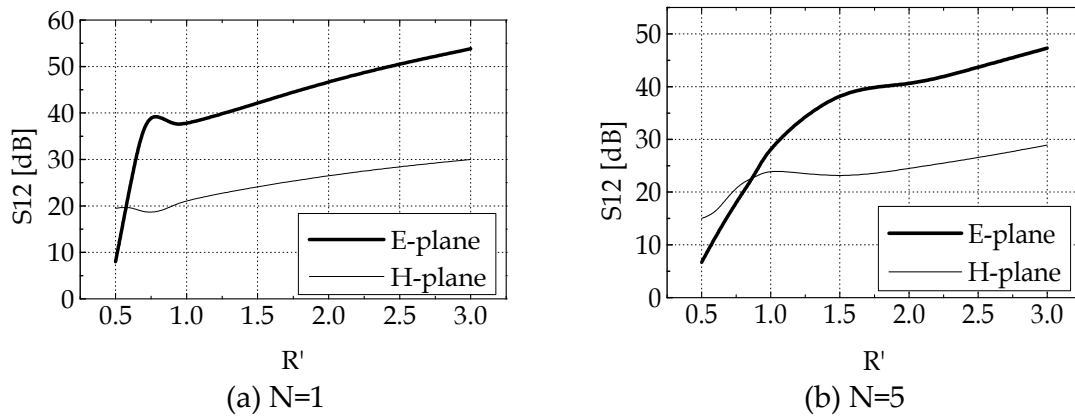
Figure 22. Isolation ratio between two antennas

E-plane   H-plane
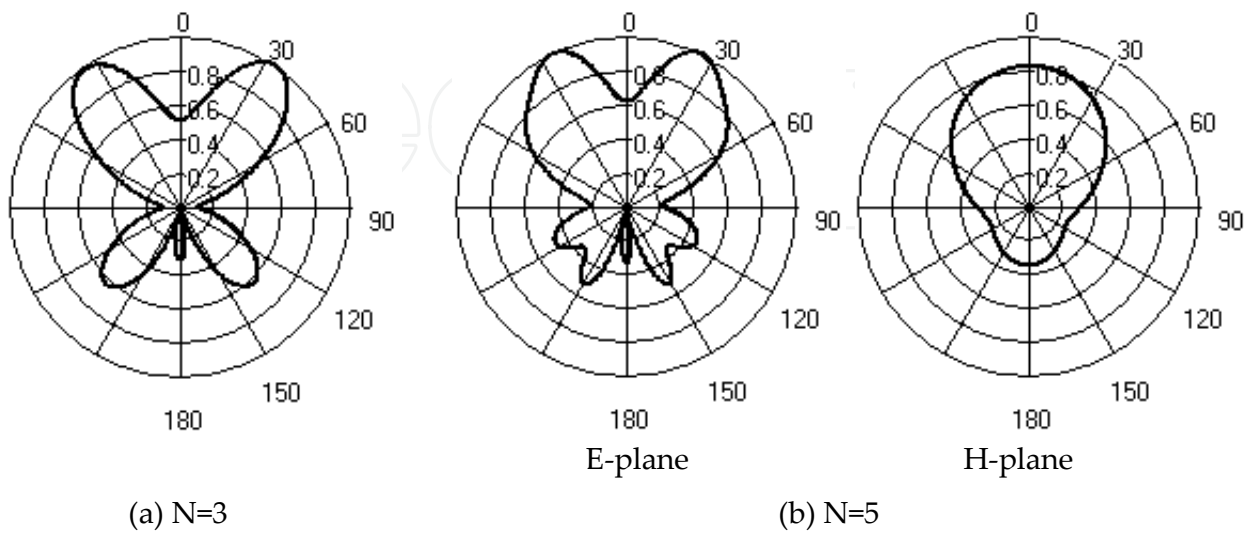
(a) N=3   (b) N=5

Figure 23. Directional pattern of director antenna as part of arc array

The influence of interaction on the directional pattern of a Yagi-Uda antenna is different in plane and convex arrays. Fig. 23 shows the directional patterns in the E-plane of a director antenna with N=1 in the arc array for the number of emitters M=3 and M=5 at a distance between emitters D=0,55 λ . The angle between the axes of the neighboring antennas is equal to β =22°. In both cases, the middle antenna is excited, the remaining ones are loaded with matched loads.

It follows from the comparison of fig. 20b, c and fig. 23b, c that, at the same linear distance between the neighboring emitters (D), the interaction between director antennas as a part of an arc array results in more considerable changes, than if they are a part of a linear array. The dependence of an isolation ratio between two director antennas on an angle between their axes of antennas (β) is shown in fig. 24 for two distances between the antennas entries D' =D/λ = 0,5 and D' =D/λ = 0,7 and two values of the number of directors N=1 and N=5.
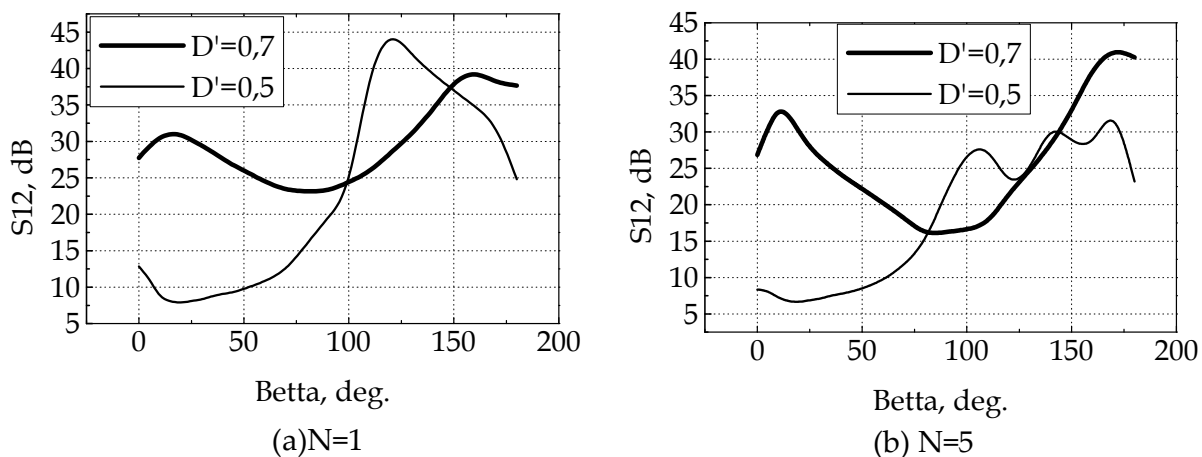

Figure 24. Dependence of isolation ratio on angle between axes of antennas

It follows from the results of numerical simulation that

1. If $D < (0,5 - 0,6)\lambda$, when an angle β increases, the isolation ratio decreases at first, then it increases and reaches a maximum at β =110°-120°.
2. If $D > (0,65 - 0,7)\lambda$, when an angle β increases, the isolation ratio increases at first, then it decreases and reaches a minimum at $\beta \approx 90°$.

3.3. Linear Antenna Array with Series Excitation

The dipole arrays of half-wave dipoles with series excitation are decribed briefly in the book [Rothammels, 1995] with the reference to the works [Brown, Liwis and Epstein, 1937; Bruckmann, 1938). Such antennas are gone by the name of Franklin antennas (Franckin C.S. – British patent № 242342, 1924). Versions of such antennas are shown in fig. 25. The drawing symbols are the following: A is half-wave dipoles: B is closed quarter-wave stubs; C is double-wire line exciting line; D is stub bonding; L is dipole length; H is stub length; d is stub width; P is point of observation in space; P₁ is projection of point P on XY plane; R, θ, ϕ are the spherical coordinates of point P.

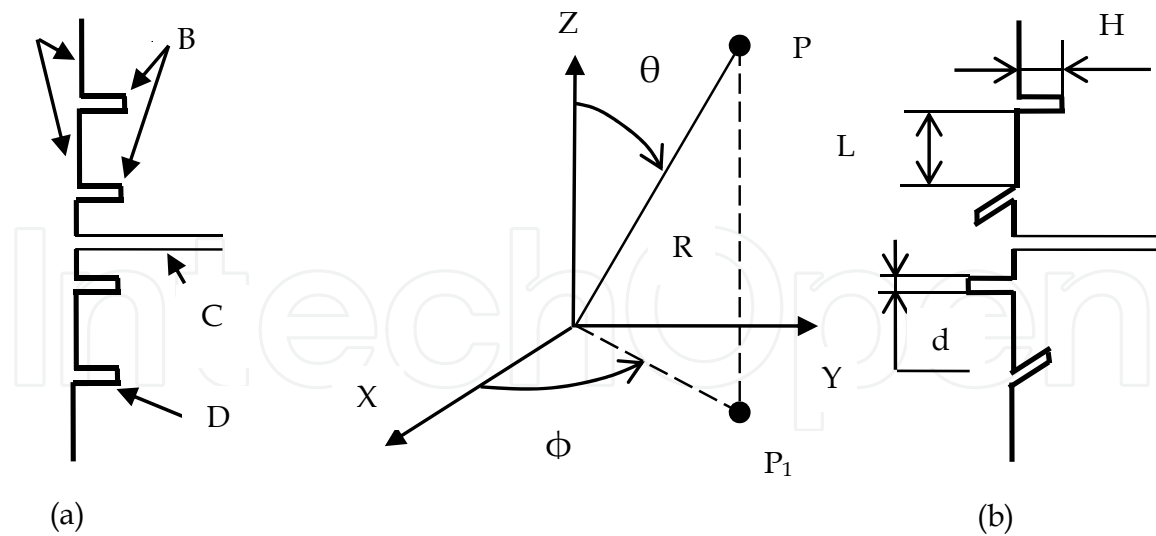**Figure 25.** Fig. 25. Franklin antennas

The polarization of an antenna radiation field is linear: the E-plane is the plane ϕ=const, the H-plane is the plane XY. In the H-plane, the directional pattern is quasi-isotropic.

Antenna characteristics depend on geometrical sizes of L, H, d, the number of dipoles in the antenna, an angle between the neighbouring stubs, frequency f. In the literature, these regularities are not studied, and they are the subject of the numerical simulation in the present chapter. Besides, in the chapter, we study the modifications of a Franklin antenna that are more wideband as for the matching criterion and have a sector-shaped directional pattern in the E-plane.

The version shown in fig. 25a at a resonance frequency, which corresponds to the equality to zero of a reactive part of an input resistance (X=0), has a high active input resistance (R). For illustration, in fig. 26, the dependences R(f) X(f) are shown for an antenna with geometrical sizes: L=0,5 λ_o ; H=0,25 λ_o ; d=0,1 λ_o , where λ_o is the medium wavelength of the given bandwidth. The calculations have been made for λ_o =300 mm (medium frequency f_o =1000 MHz) and two cases with the number of dipoles N=3 and N=5. It is evident that at N=3, there is a frequency, at which X=0. At N$\geq$5, there is no such a frequency (X <0). It complicates the antenna matching with a transmission line.

The more convenient version for matching is the one, in which the exciting voltage is introduced into a bonding rupture. Such a version is shown conditionally in fig. 27. The place of the antenna excitation is marked by a big point. The dependences R(f) and X(f) are shown in fig. 28 a. In such an antenna, the choice of values L, H, d can be X=0, and R=50 Ohm or 75 Ohm. The graphs of fig. 28 correspond to the antenna tuning to a frequency of 1000 MHz in order to obtain R=50 Ohm, X=0 (L=142 mm; H=71,5 mm; d=8 mm). The symbols of R and X are the same as in fig. 26.

The numerical simulation shows that with increase of the number of dipoles in the antenna (N), the antenna band properties worsen. The VSWR minimum does not match to the most

acceptable directional pattern in the E-plane. Fig. 29 shows the directional patterns at three frequencies of the band, in which VSWR<2. The frequency values, gain (G), R, X, VSWR are also given. The graphs of directional patterns in the H-plane give the values of nonuniformity of the directional pattern (Nu). The nonuniformity Nu decreases, if to direct the neighbouring stubs in the contrary directions (fig. 25b).
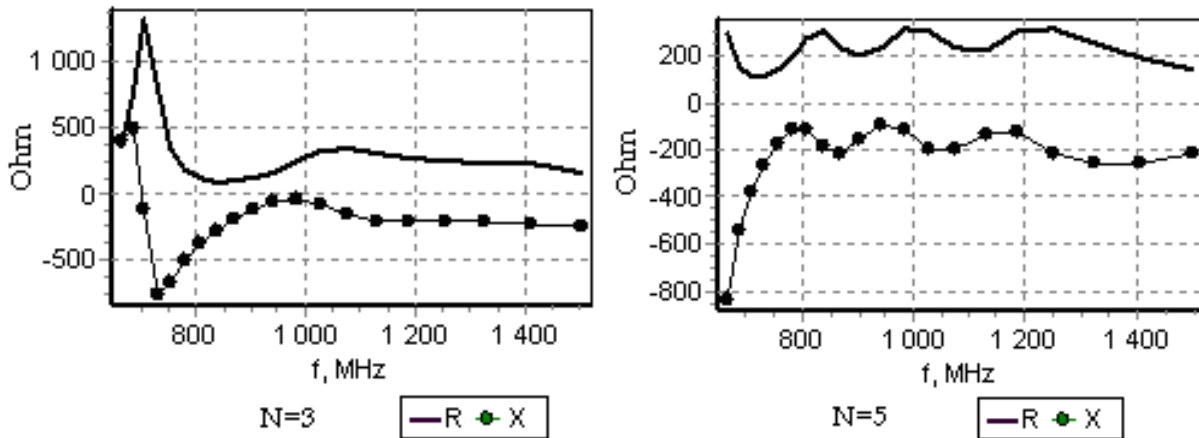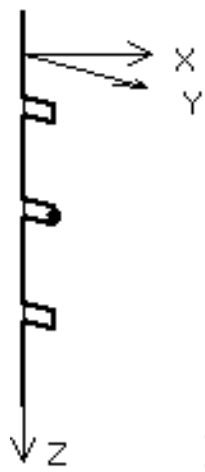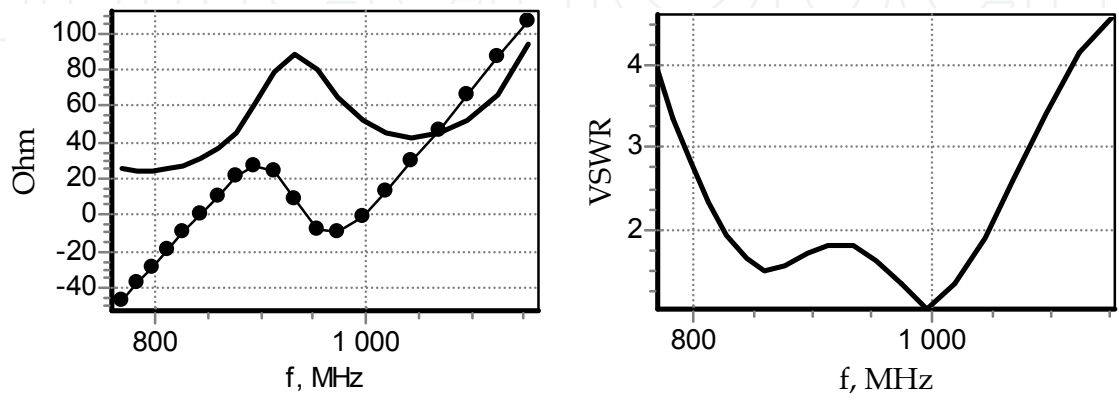
Figure 26. Dependences of input resistance on frequency

Figure 27. Antenna

Figure 28. Input resistance and VSWR in bandwidth

Antenna characteristics depend on a number of an excited stub. In fig. 27, the central stub is excited. If to displace an excitation point from the central stub, the maximum of a directional pattern in the E-plane declines from a normal to the Z axis. Fig. 29 illustrates these properties by the example of the antenna with N=6. When the frequency increases, the angle of deflection of the maximum of a directional pattern decreases. Fig. 30 shows the DP of the antenna with N=13 within a bandwidth, in which VSWR<2. The lower stub is excited, as in fig. 29. The band of matching frequencies depends little on the number of dipoles in the antenna, if the extreme stub is excited. For illustration, fig. 31 shows the dependence of VSVR(f) at different values of the number of dipoles.

When the number of dipoles increases, the misphasing between the stub that is excited and the extreme stubs increases. Therefore, when the number of dipoles increases, the antenna gain at first increases promptly, then slowly. The dependence of gain (G) on the number of dipoles is shown in fig. 32. At N=1, the antenna represents a half-wave dipole that has G=2 dB. The lower stub is excited in the antenna. It follows from fig. 32 that there is no sense to make the number of dipoles N> 5.
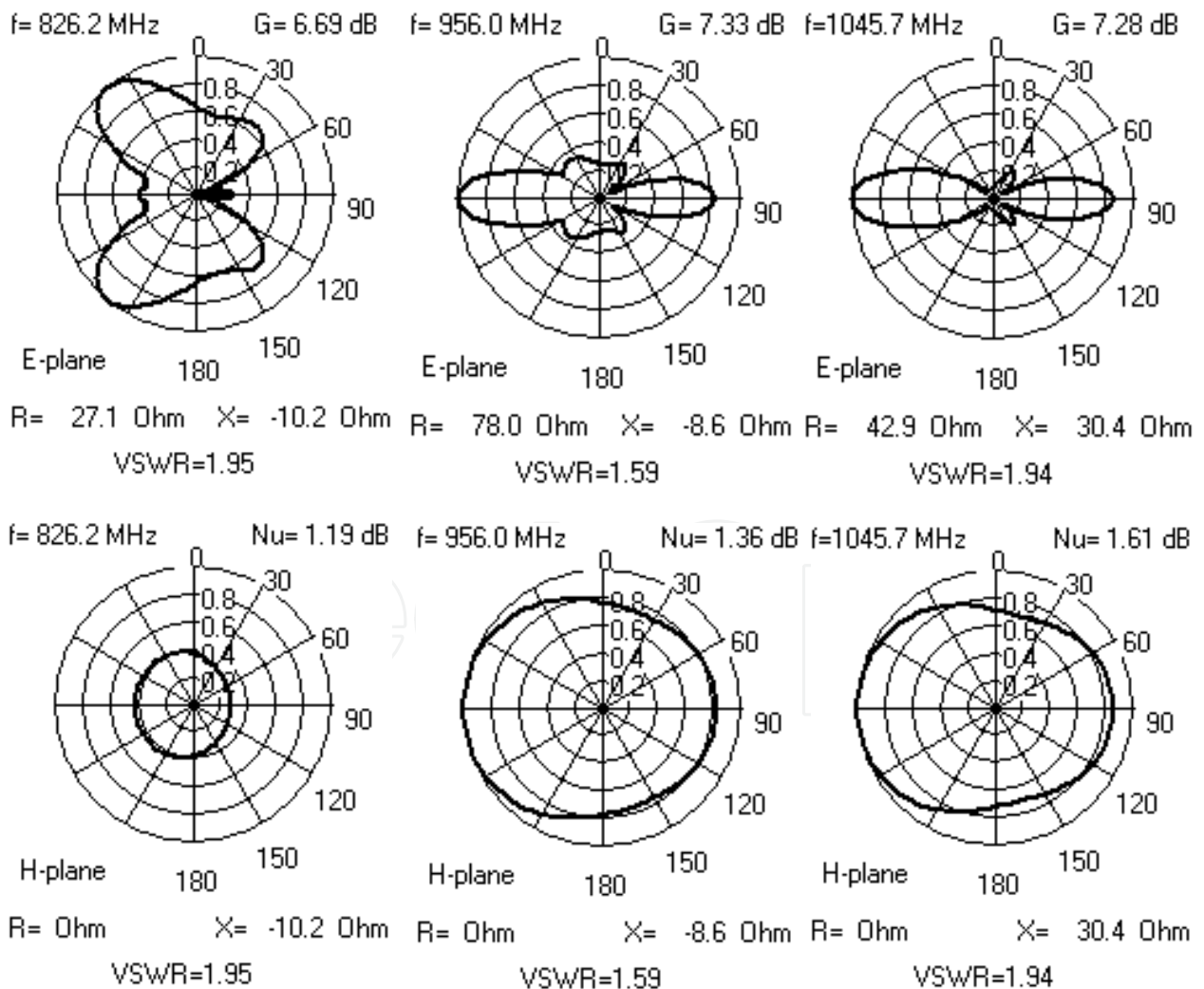

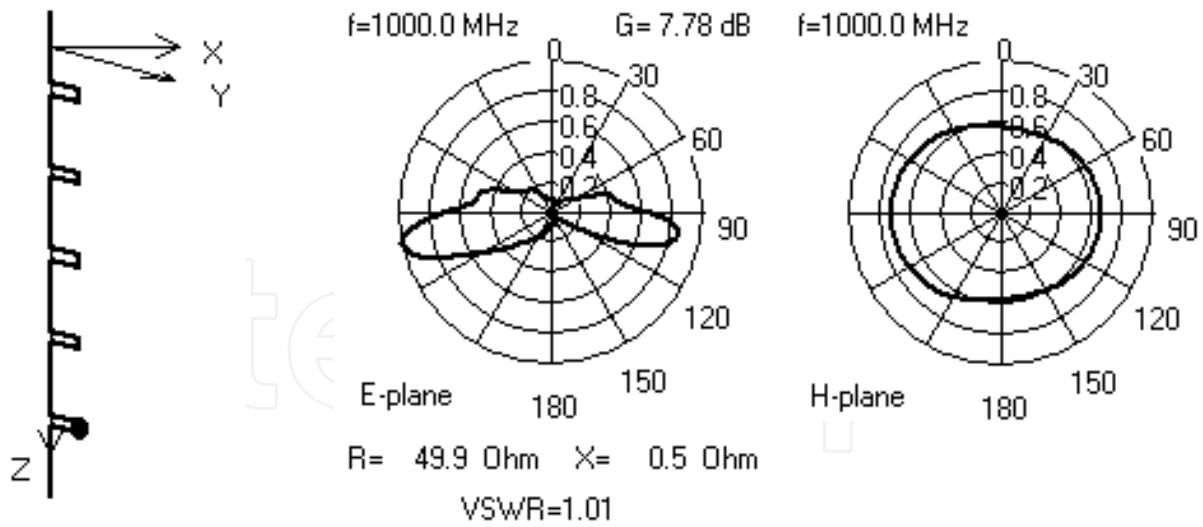**Figure 29.** Directional patterns in E and H-planes

f=1000.0 MHz   G= 7.78 dB   f=1000.0 MHz

E-plane

H-plane

R=   49.9 Ohm   X=   0.5 Ohm

VSWR=1.01

Figure 30. Nonsymmetric excitation of antenna

f=1047.8 MHz   G= 7.70 dB   f=1010.6 MHz   G= 7.92 dB   f= 913.5 MHz   G= 8.03 dB

E-plane   E-plane   E-plane

R=   49.3 Ohm   X=   27.4 Ohm   R=   49.6 Ohm   X=   5.8 Ohm   R=   56.6 Ohm   X= -36.8 Ohm

VSWR=1.73   VSWR=1.12   VSWR=1.99
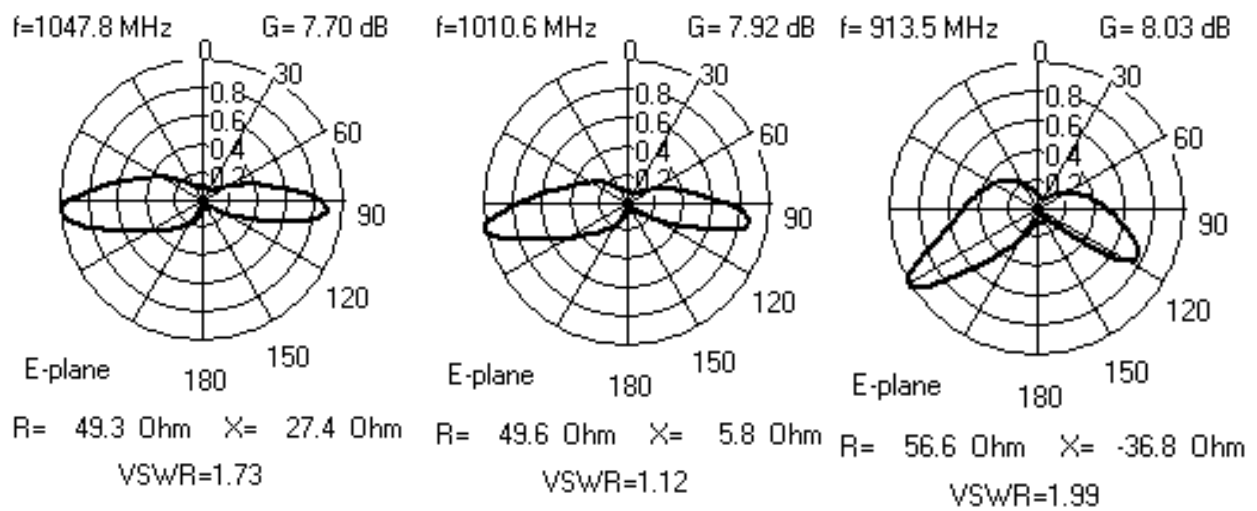
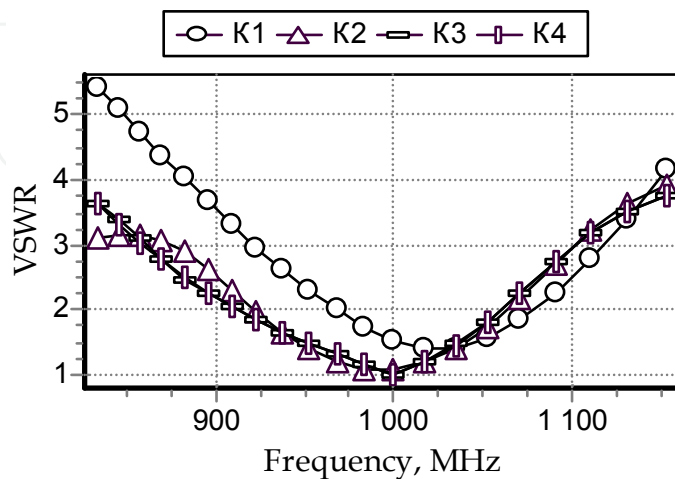**Figure 31.** Directional patterns within bandwidth: N=13, the lower stub is excited.

Figure 32. Dependence of VSWR on frequency
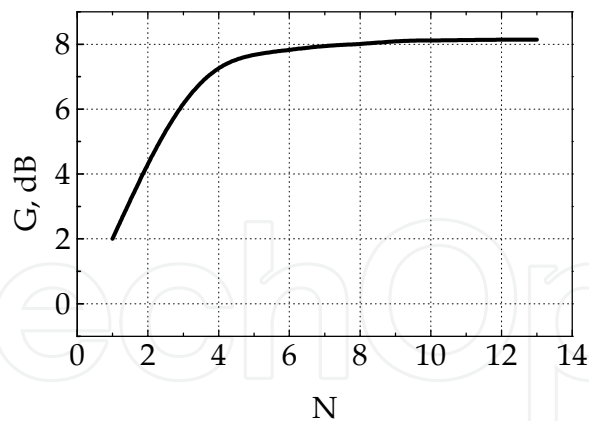K1 – N=2; K2 – N=4; K3 – N=7; K4 – N=13

Figure 33. Dependence of Gain on number of dipoles

K1 – N=2; K2 – N=4; K3 – N=7; K4 – N=13

If to apply a system of reflectors or (and) directors to an antenna, it is possible to make a directional pattern sector-shaped in the H-plane. Fig. 33 shows such an antenna and its directional pattern.

A Franklin antenna and its modifications can be used as transmitting antennas in radio links.

4. Modelling of radiation and scattering characteristics of frame antennas

4.1. Loop antenna of closed and open arrays

Various types of loop antennas are used in radio communication, radiolocation, TV. Further in this chapter, two types of loop antennas are studied: on the basis of closed arrays with a lateral length $L \approx 0,25\lambda$ (fig.34a) and on the basis of open arrays with a lateral length $L \approx 0,5\lambda$ (fig.34b). Double loop antennas and arrays of such antennas are studied. The double loop antennas are used with a reflector (fig.34c) and without a reflector. The distance between the plane of the array and the reflector is H.

The polarization of the antenna is linear. The E-plane is the XY plane, the H-plane is the plane φ=const. The antenna characteristics depend on geometrical sizes of L, β, d, Le, Lh, Dh, H. The antenna is excited by voltage between points 1 and 2. In version (a), the resistance between points (input resistance of the antenna) can be made equal to 50 Ohm, in version (b) – an active part of the input resistance – 200-300 Ohm. Gain in the version (b) of the antenna is 3 dB bigger, than in the version (a) of the antenna. In versions (a) and (b), directors can be used to increase the gain, fig. 35.

In the literature, the methods of antenna excitation were studied, their key properties were studied briefly [Rothammels K, 1995], but there is no information about the main regularities. Further, these regularities are examined for version 34a only, because this version is generally used.
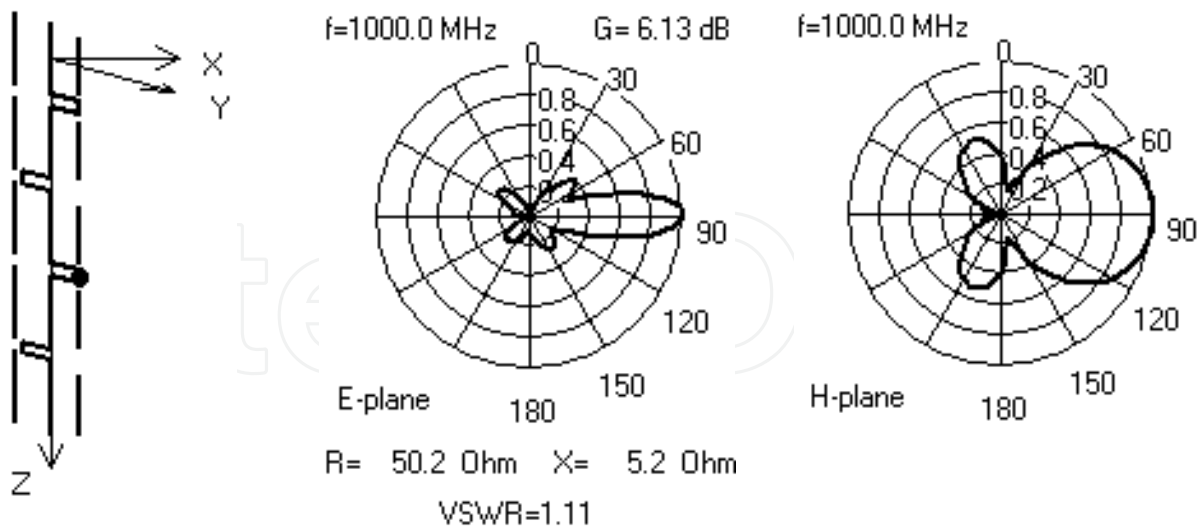
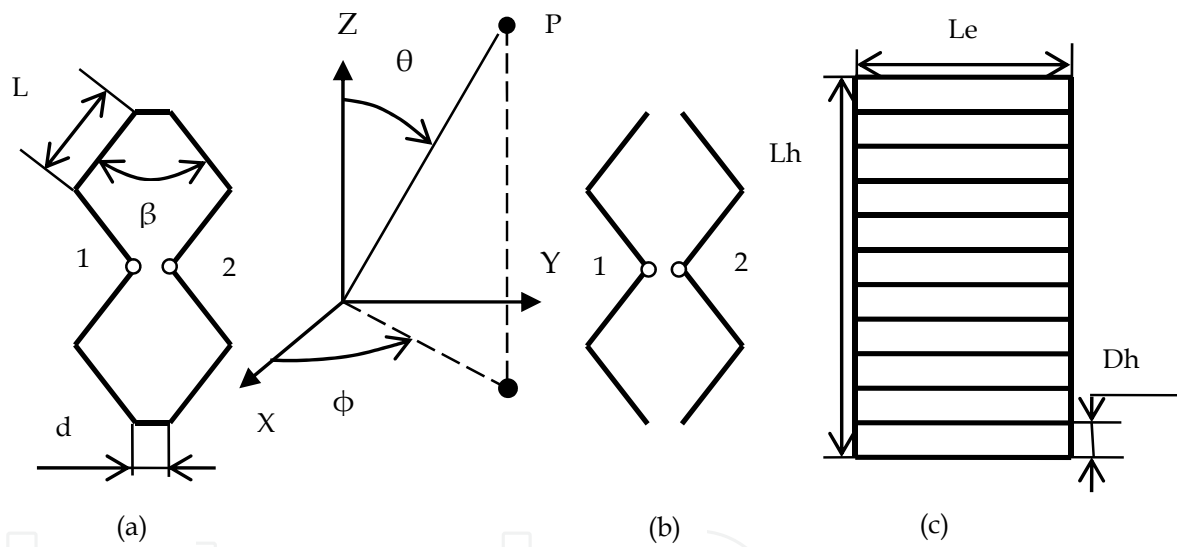**Figure 34.** Franklin antenna with linear reflectors and directors

(a)   (b)   (c)
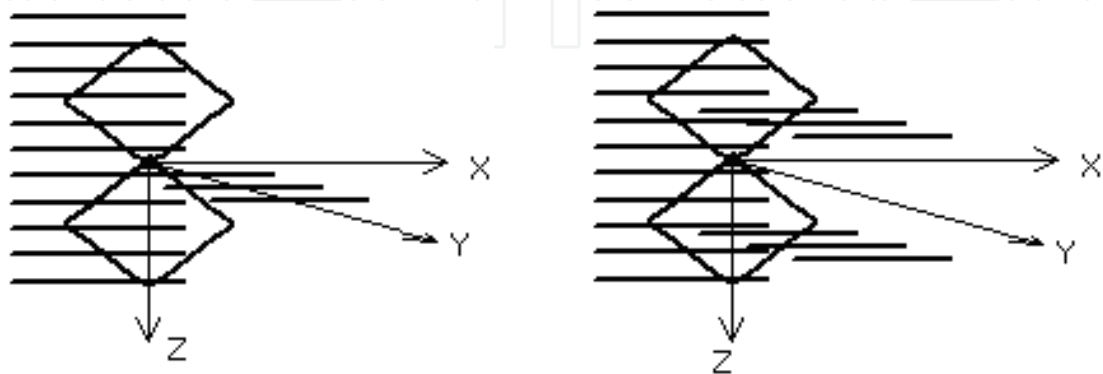
Figure 35. Loop antennas

Figure 36. Loop antennas with directors

Fig. 36a shows the dependence of an active part of an input resistance (R) on an angle β, if a reactive part of the input resistance is equal to zero ($X \approx 0$). The condition $X \approx 0$ is met by changing a lateral length of an array (L) for each preset value of $H' = H/\lambda$. Fig. 36b shows the dependence of $L' = L/\lambda$ on an angle β (values of L' meet the condition $X \approx 0$). The calculations have been made for the antenna with a wire diameter of Do=0,006 λ, d=0,006 λ.
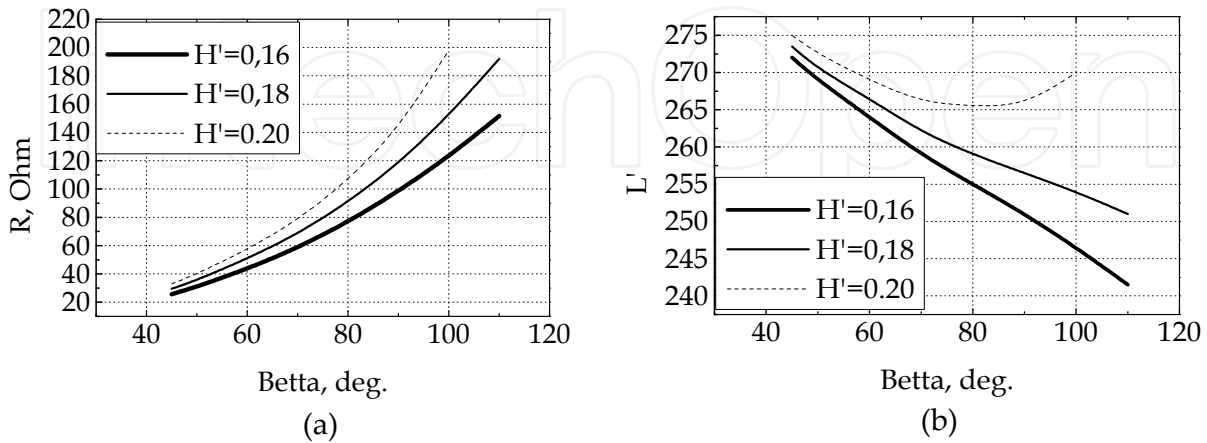

Figure 37. Dependence of input resistance (a) and array lateral length (b) on angle β

It follows from fig. 36a that, by selecting the values of L and β at preset H, it is possible to make input resistance R preset and to meet the condition $X \approx 0$.

The antenna band properties are illustrated by fig. 37, 38. The calculation has been made for the antennas calculated so that at a frequency of 300 MHz the input resistance was equal to $R \approx 50$ Ohm, $X \approx 0$, see fig. 37a, and $R \approx 75$ Ohm, $X \approx 0$, see fig. 37b. Fig. 38a shows the dependence of VSWR on frequency. For antenna 1 with the input resistance of 50 Ohm at a frequency of MHz, VSWR has been calculated in a line with the characteristic resistance of 50 Ohm (graph 1), for antenna 2 with the input resistance of 75 Ohm, VSWR has been calculated in a line with the characteristic resistance of 75 Ohm (graph 2). It is evident that the antenna with a higher input resistance is matched to a bigger bandwidth. Fig. 38b shows the dependences of gain and F/B parametre for the second antenna.
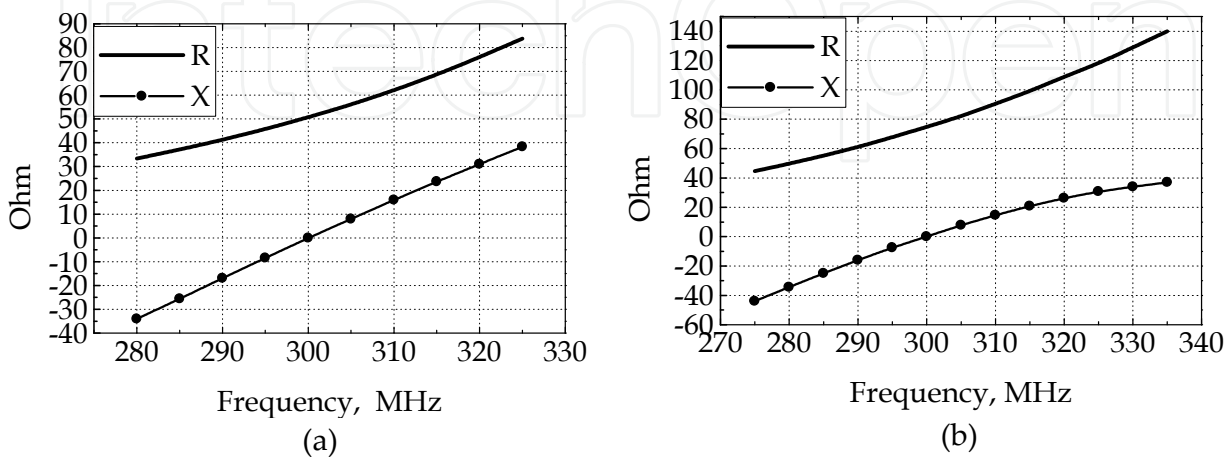

Figure 38. Dependence of input resistance on frequency

It follows from the results of the numerical simulation, that at a level of VSWR<2, the percentage bandwidth is $\delta f = (f_{max} - f_{min}) / f_o \cdot 100 \approx (10\text{-}20)\%$. The values of Gain and F/B in the said bandwidth vary little. The matched bandwidth increases, if R increases at a medium frequency. To widen the matched bandwidth, additional elements are used in the loop antenna.
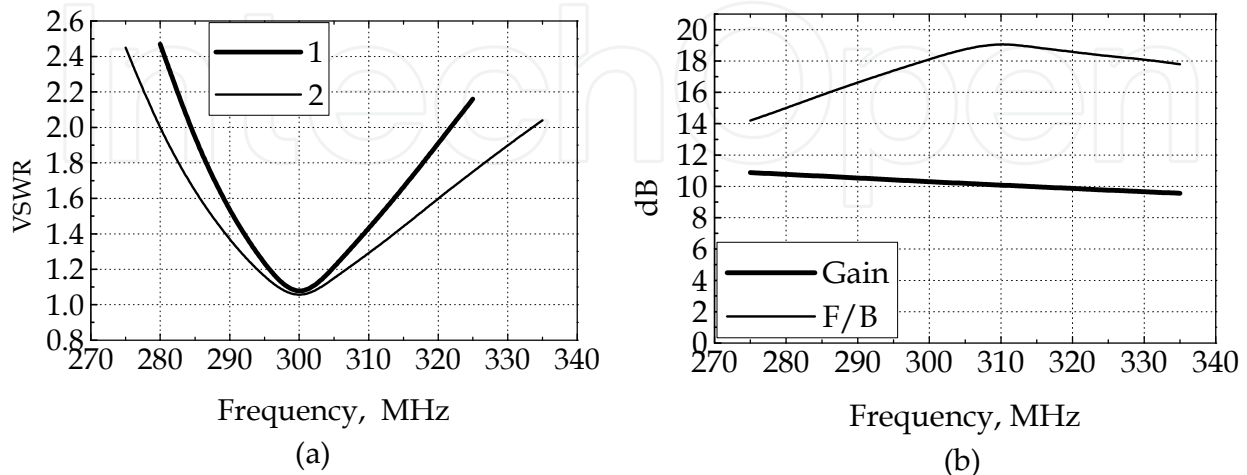

Figure 39. Dependence of VSWR, Gain and F/B parametre on frequency

4.2. Interaction of loop antennas as part of antenna array

Interaction of loop of antennas as a part of an array results in changing of their characteristics. It shall be taken into consideration, when designing antenna arrays. Fig. 39 shows directional patterns in the E and H-planes of a loop antenna with an input resistance of 50 Ohm: isolated one (a); when taking into account its interaction with two neighbouring emitters – one on the left and one on the right (b); and taking into account its interaction with four neighbouring emitters – two on the left and two on the right. The values of input resistance, gain and parametre F/B are also shown in the figures. The calculations have been made for a linear array, in which emitters are located in the E-plane, at a frequency of 300 MHz (as an example). The distance between the neighbouring emitters is equal to 0,65λ. It follows from the results of simulation that the interaction influences an input resistance and F/B parametre insignificantly. The directional pattern and gain influence the interaction greatly, but differences in influence of various number of interacting loop antennas are insignificant (fig.39b and 39c). It means that when simulating multiple-unit arrays of loop antennas, it is possible to take into consideration interaction of each emitter only with its nearest emitters, and further to use the theorem of multiplication of directional patterns.

Fig. 40 illustrates difference in influence of interaction in a linear array and in an annular array. The figure shows directional patterns of a loop antenna with the same geometrical sizes without taking interaction into consideration (a), when taking interaction into consideration with two neighbouring emitters (b), and with four neighbouring emitters (c). The linear distance between the neighbouring emitters is equal to 0.65λ, the angle between axes of antennas is equal to 12°.
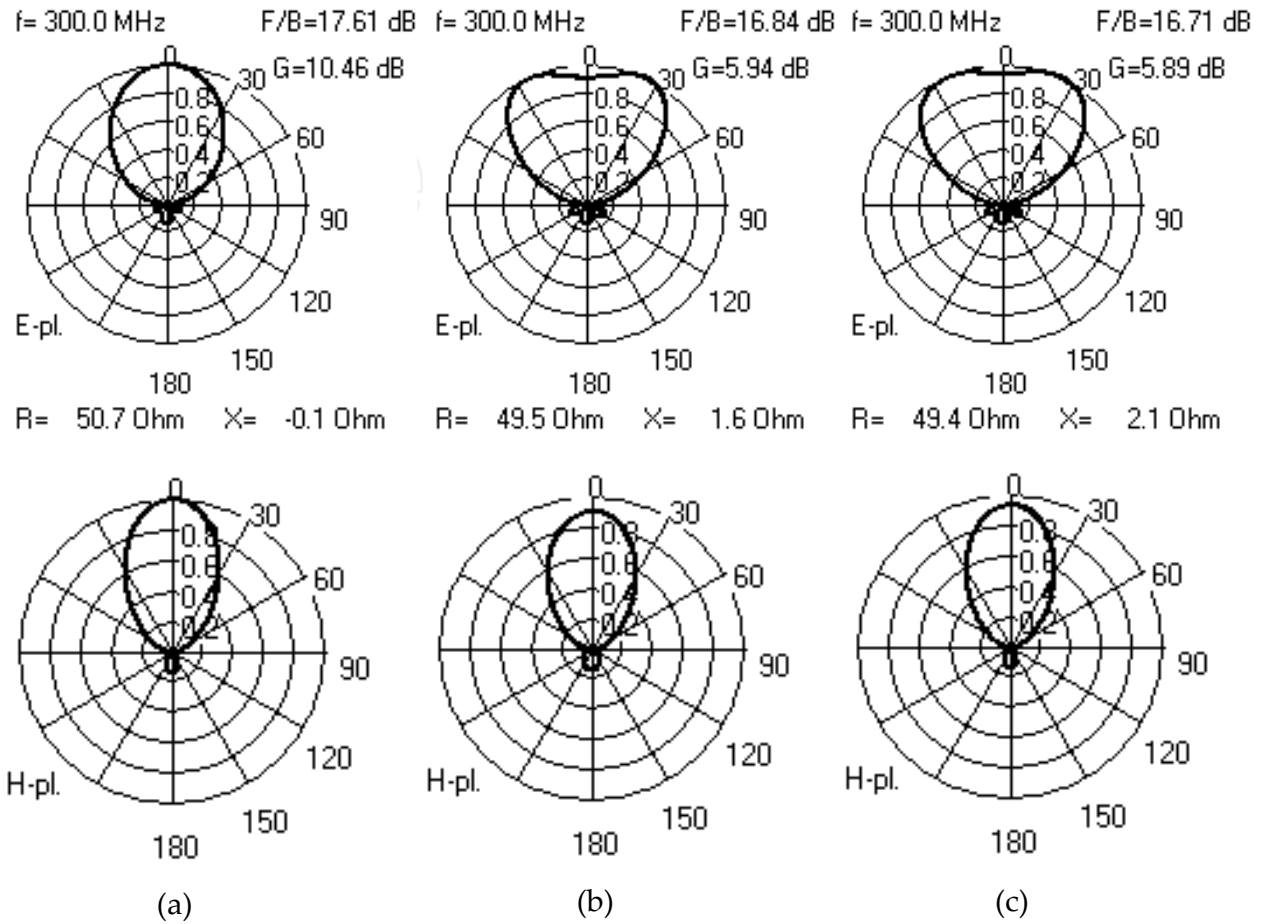
Figure 40. Loop antenna directional patterns (a) and when taking into consideration its interactions as a part of a linear array (b), (c).

It follows from the comparison of fig. 39 and fig. 40 that interaction between loop antennas in an annular array is less than interaction in a linear array.

4.3. Linear antenna arrays with coherent excitation

To increase gain, it is possible to use linear arrays of loop antennas with series excitation. Fig. 41 shows the schema of connections of arrays among themselves at a lateral length of the array $L \approx 0,25\lambda$ (a) and at a lateral length of the array $L \approx 0,5\lambda$ (b) by the example of the antennas with Mp=4. The gain increases, if the number of the arrays increases due to narrowing of the main lobe in the H-plane. Fig. 42 shows the dependence of the gain on the

number of Mp arrays at $L \approx 0,25\lambda$. Fig. 42b illustrates the dependence of the input resistance on the number of arrays. The sizes of elements of the arrays are chosen so that the input resistance was equal to 50 Ohm at Mp=2.
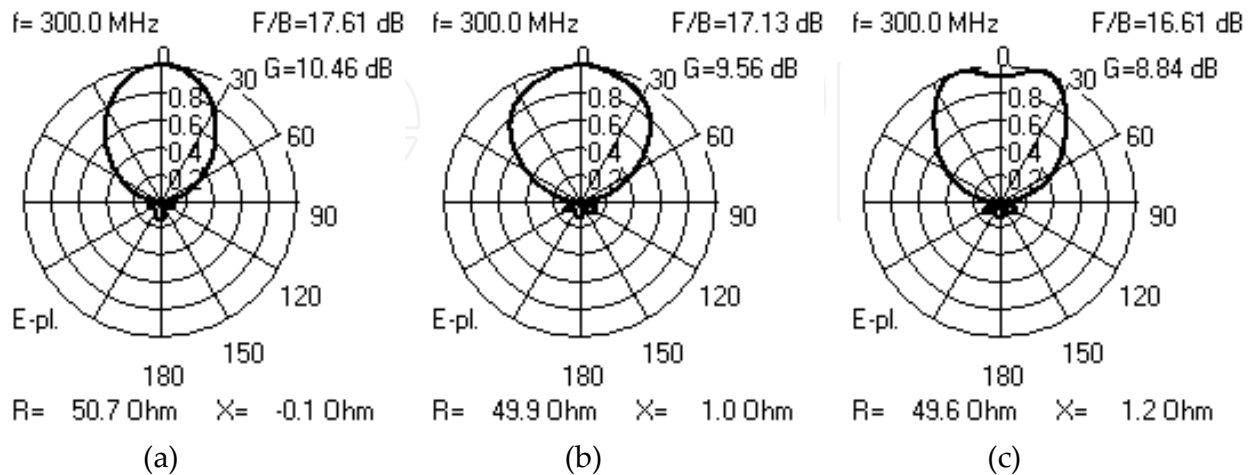
Figure 41. Directional patterns of a loop antenna, when taking into consideration its interaction as a part of an annular array
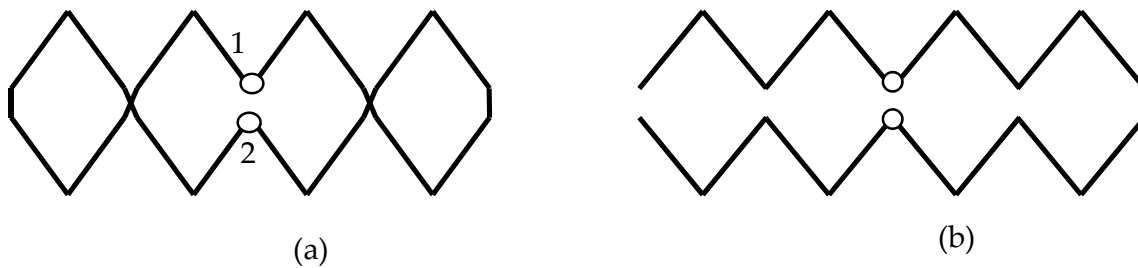
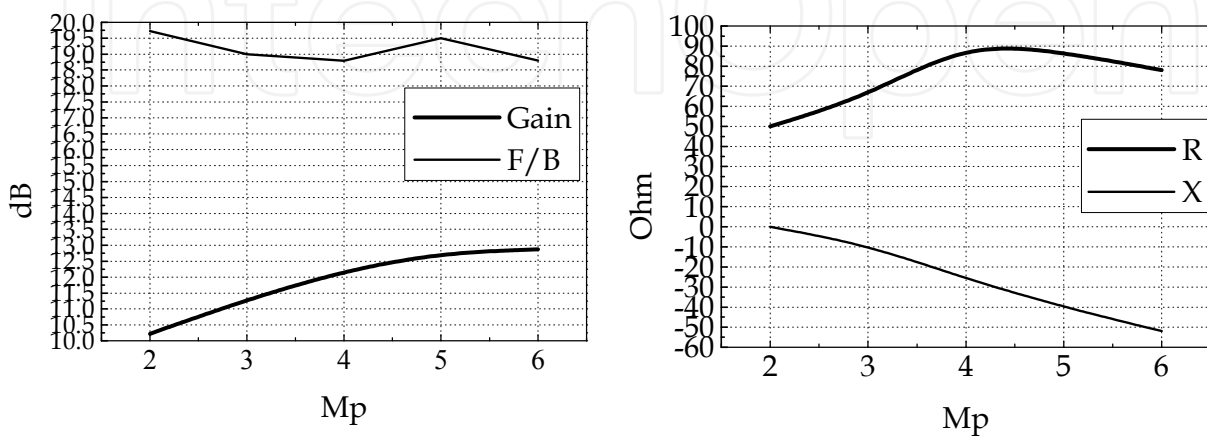**Figure 42.** Connecting pattern of arrays in linear array

Figure 43. Dependence of parametres of a loop antenna on the number of arrays at $L \approx 0,25\lambda$

It follows from the results of simulation that it is not reasonable to make Mp>4 in the antenna. For each M value, it is necessary to optimise the sizes of elements of arrays in order to obtain the preset input resistance.

In a linear array consisting of arrays with a lateral length $L \approx 0,5\lambda$, the gain is 3 dB more approximately.

Fig. 43a shows the version of a linear array with a quasi-isotropic directional pattern in the E-plane. Such a pattern can be obtained, if to bend all the arrays along the Z axis at an angle α =35-40°. It is possible to ensure the preset input resistance by choosing the sizes of elements. Fig. 43b,c shows the directional patterns and the values of the parameters of G (Gain), NR (nonuniformity of a directional pattern in the E-plane), R, X, values of VSWR in a line with a wave resistance of 50 Ohm.
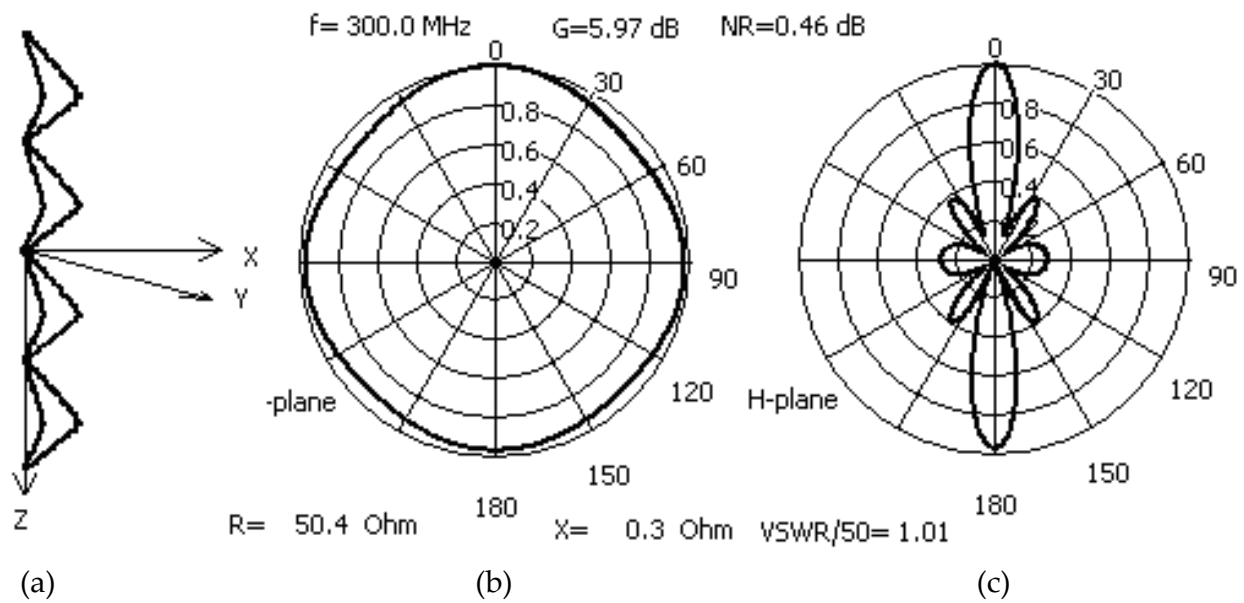

(a)   (b)   (c)

Figure 44. Loop antenna with quasi-isotropic directional pattern in E-plane

5. Conclusion

The simulation results, given in this chapter, complete the information about dipole and loop antennas that is available in the literature, and can be used to choice a type of an antenna according to specified requirements and after estimating its main characteristics. Numerical simulation of an antenna can be done with the use of the formulas given in the description of a mathematical model. When using a program developed on the basis of these formulas, it is necessary to carry out research into the convergence of the results of calculation. The most sensitive parametre of the antenna in relation to the number of segments of division of conductors (M) is the input resistance. When using impulse functions as the basis and weight ones, it is possible to be oriented towards the following recommendations: the ratio of a segment length to a conductor diameter $\Delta L / 2Ao \approx 0,8$-$1,2$; the number of segments at a wavelength: 80-200.

In some cases, the results given in the graphs can be used directly with the use of electrodynamic scaling.

We express aur gratitude to D.Moskalev and V.Kizimenko for the useful discussion of the results described in this chapter.

Author details

Oleg A. Yurtsev and Grigory V. Ptashinsky
Belarusian State University of Informatics and Radioelectronics, Belarus

6. References

Antenna Theory. (1997). Analysis and design. Second Edition Balanis, C.A. John Wiley&Sons. Inc.

Aisenberg, G.Z, Jampolsky, V.G. and Terjoshin, O.N. (1977). *Antennas UHF*. M.Svjaz. Russia.

Brown, G.H., Epstein, J and Liwis, R.F. (1937). Groud System as a Factor in Antenna Efficiency.//Proc. IRE, June 1937, pp.753-787.

Bruckmann, H. (1938).*Uber die Theorie der Erdvarluste von Antennen.*//TFT 27, H.2 pp.29-38.

Crispin, J.W., Maffett A.L.(1965). *Radar Cross-Section Estimation for Complex Shapes*.//Proceeding of the IEEE. −Vol. 53. − № 8. − 1965. pp.1115-1125.

Computer Techniques for Electromagnetics. Edition by Mittra, R. (1973). Pergamon Press. New York.

Drabkin, A.L. and Zuzenko, V.L. (1961). *Antenna-feeder devices*. M. Sovetskoe radio. Russia.

Franckin, C.S. (1924). British patent № 242342.

Fletcher, C.A.J. (1984). *Computational Galerkin method*. Springer-Verlag, New York.

Fradin, A.Z. (1977). *Antenna-feeder devices*. M.Sviaz. Russia.

Harrington, R.F. (1968). *Field Computating by Moment Methods*. Macmillan, New York.

Markov, G.T. (1960). *Antennas.* M.-L. Gosenergoizdat. Russia.

Radar Handbook.(1970). M.I.Skolnik. EDITOR - IN - Chief. Mc Graw-Hill Company, 1970.

Rothammels, K. (1995). *Antennenbuch.* Franckh-Kosmos. Verlags-GmbH&Co., Stuttgart.

Sazonov, D.M and Shkolnikov, A.M. (1974).*The scattering of electromagnetic waves by a loaded antenna array*//Radiotechnology and Electronics. −1974. − № 4. pp.689-686.

Stratton, J.A. (1941). *Electromagnetic Theory*. McGraw-Hill.

Volakis, J.L. (2007). *Antenna Engineering Handbook*. Mc Graw-Hiil Companies.

Kazarin, A.N. , Runov, A.V. and Yurtsev, O.A. (1974). *Helix Antennas*. M. Sovetskoe radio. Russia.